



Soil-Powered Computing: The Engineer's Guide to *Practical Soil Microbial Fuel Cell Design*

BILL YEN and **LAURA JALIFF**, Northwestern University, USA

LOUIS GUTIERREZ, UC San Diego, USA

PHILOTHEI SAHINIDIS, Georgia Institute of Technology, USA

SADIE BERNSTEIN, Northwestern University, USA

JOHN MADDEN, **STEPHEN TAYLOR**, and **COLLEEN JOSEPHSON**, UC Santa Cruz, USA

PAT PANNUTO, UC San Diego, USA

WEITAO SHUAI, **GEORGE WELLS**, and **NIVEDITA ARORA**, Northwestern University, USA

JOSIAH HESTER, Georgia Institute of Technology, USA

Human-caused climate degradation and the explosion of electronic waste have pushed the computing community to explore fundamental alternatives to the current battery-powered, over-provisioned ubiquitous computing devices that need constant replacement and recharging. Soil Microbial Fuel Cells (SMFCs) offer promise as a renewable energy source that is biocompatible and viable in difficult environments where traditional batteries and solar panels fall short. However, SMFC development is in its infancy, and challenges like robustness to environmental factors and low power output stymie efforts to implement real-world applications in terrestrial environments. This work details a 2-year iterative process that uncovers barriers to practical SMFC design for powering electronics, which we address through a mechanistic understanding of SMFC theory from the literature. We present nine months of deployment data gathered from four SMFC experiments exploring cell geometries, resulting in an improved SMFC that generates power across a wider soil moisture range. From these experiments, we extracted key lessons and a testing framework, assessed SMFC's field performance, contextualized improvements with emerging and existing computing systems, and demonstrated the improved SMFC powering a wireless sensor for soil moisture and touch sensing. We contribute our data, methodology, and designs to establish the foundation for a sustainable, soil-powered future.

CCS Concepts: • **Hardware** → **Energy generation and storage**; • **Human-centered computing** → **Empirical studies in ubiquitous and mobile computing**; • **Computer systems organization** → **Embedded and cyber-physical systems**.

Additional Key Words and Phrases: Microbial Fuel Cells, Energy Harvesting, RF Backscatter

ACM Reference Format:

Bill Yen, Laura Jaliff, Louis Gutierrez, Philothei Sahinidis, Sadie Bernstein, John Madden, Stephen Taylor, Colleen Josephson, Pat Pannuto, Weitao Shuai, George Wells, Nivedita Arora, and Josiah Hester. 2023. Soil-Powered Computing: The Engineer's Guide to *Practical Soil Microbial Fuel Cell Design*. *Proc. ACM Interact. Mob. Wearable Ubiquitous Technol.* 7, 4, Article 196 (December 2023), 40 pages. <https://doi.org/10.1145/3631410>

Authors' addresses: **Bill Yen**, billyen2023@u.northwestern.edu; **Laura Jaliff**, laurajaliff2025@u.northwestern.edu, Northwestern University, Illinois, USA; **Louis Gutierrez**, UC San Diego, California, USA, lsgutierrez@ucsd.edu; **Philothei Sahinidis**, Georgia Institute of Technology, Georgia, USA, philothei@gatech.edu; **Sadie Bernstein**, Northwestern University, Illinois, USA, sadiebernstein2023@u.northwestern.edu; **John Madden**, jtmadden@ucsc.edu; **Stephen Taylor**, sgtaylor@ucsc.edu; **Colleen Josephson**, cjosephson@ucsc.edu, UC Santa Cruz, California, USA; **Pat Pannuto**, UC San Diego, California, USA, ppannuto@ucsd.edu; **Weitao Shuai**, weitao.shuai@northwestern.edu; **George Wells**, george.wells@northwestern.edu; **Nivedita Arora**, nivedita@northwestern.edu, Northwestern University, Illinois, USA; **Josiah Hester**, josiah@gatech.edu, Georgia Institute of Technology, Atlanta, USA.



This work is licensed under a Creative Commons Attribution-NonCommercial International 4.0 License.

© 2023 Copyright held by the owner/author(s).

2474-9567/2023/12-ART196

<https://doi.org/10.1145/3631410>

1 INTRODUCTION

As the consequences of climate degradation become increasingly prominent, it is imperative for society to find sustainable alternatives to power our ever-growing need for computation. Soil Microbial Fuel Cells (SMFCs) are a promising source of renewable energy in applications where regular chemical batteries and solar panels fall short, such as in green infrastructures, wetlands, or underground. Solar panels are prone to getting covered by dirt or foliage in wet locations with vegetation and do not work at night, while batteries contain contaminants that may leach into the environment if they were not retrieved [46]. Furthermore, they both require high-impact minerals like tin and cobalt that impose heavy negative externalities on the environments they are harvested from [41]. SMFCs generate power using the naturally occurring microbes in their environment. They can be made from many types of locally sourced, biomass-based materials with significantly smaller, if not negative, carbon footprints [62]. They can also be deployed almost anywhere there is soil and are highly scalable since they do not require raw materials with complex external supply chains like lithium or silver. SMFCs have been demonstrated to produce as much as 200 μW of power with an open-circuit voltage upwards of 731 mV [45, 86] under optimal, carefully-controlled conditions. This theoretically makes SMFCs a viable option in solving the critical bottleneck in expanding the growth of smart cities and farms: the lack of decentralized, long-term, and renewable power. Overcoming this restriction will push the ubiquitous computing community closer to batteryless computational devices capable of perpetual deployment, which would enable reliable real-time monitoring of various environmental conditions (see Figure 1) that could then be used to drive policy and engineering decisions.

While the promises of SMFCs are very real, the reality of their performance outside of the lab is not ideal. The concept of microbial fuel cells has existed since 1911 [77], but their highly variable power output has hindered the computing community from making practical use of them. SMFCs are susceptible to changes in environmental conditions, with soil moisture being a particularly strong limiting factor [92, 101]. This makes efforts to deploy true terrestrial SMFCs as energy sources in the field an ongoing challenge, with no current example of a SMFC that can generate consistent amounts of power long-term outside of inundated conditions. Although there have been attempts to improve SMFC design, there is an absence of reliable comparative studies in the literature regarding the effects of cell designs on power output and their resiliency to changes in soil moisture.

As SMFCs are heavily affected by environmental conditions, types of soil, and the microbial communities that inhabit them [92], any evaluation done outside of direct comparisons in the same environment holds little meaning. While many novel SMFC designs have been proposed, they are rarely tested against each other systematically to identify their relative strengths and weaknesses. To resolve this roadblock in the development of this sustainable energy source for ubiquitous computing, we uniquely explore the SMFC design space in a principled manner and extract general design guidelines from a 2-year-long iterative design process with a combined nine months of SMFC deployment data. This iteration process spans four separate experiments and examines the relative performances of 4 distinct SMFC configurations in a common environment (see Section 3).

Our experimental framework utilizes fundamentals of electrochemistry and MFC theory and led to a design that enables stable operation under soil with 4% lower volumetric water content (VWC) than the minimum VWC required for benchmark cells, which increases SMFC's applicability in grasslands and wetlands with seasonal swings in soil moisture [25]. This greater operational moisture range translates to 40% more computing operations in simulation for digital systems and a 120% increase in theoretical runtime for analog sensors throughout its 161-day lab deployment (see Section 5.1). We further evaluated the feasibility of this new SMFC design with a combination of an outdoor deployment in real-world settings and bench-scale studies powering an analog backscatter sensor [11].

Contributions. The main contribution of this paper is an experimental framework for SMFC design iteration, which takes the first step to fill a community need for SMFC-powered computing and enables researchers to explore this new form of ubiquitous power. Specifically:

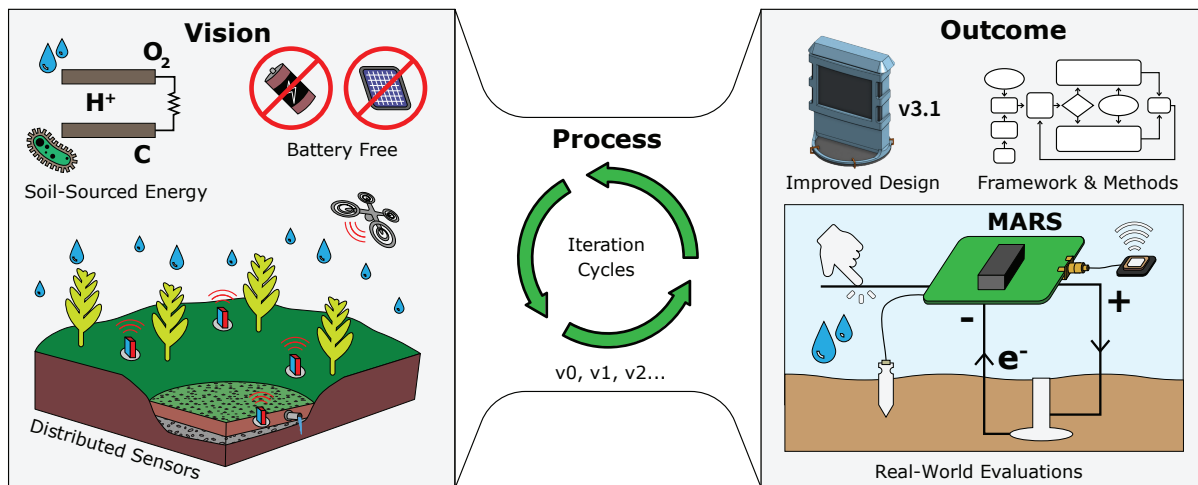


Fig. 1. Iterative design process that took the vision of sustainable, soil-powered distributed sensor networks to produce an improved SMFC prototype and methods for future researchers. We further conduct real-world evaluations on the feasibility of SMFCs as energy sources with an outdoor deployment and by integrating SMFCs with low-power analog wireless sensors.

- (1) **SMFC as Power Source:** We introduce and explain the operation of an SMFC from the perspective of its use as an energy source for computational sensing systems and the confluence of factors that finally make this century-old concept relevant for practical usage in computing. We review the state-of-the-art designs of SMFCs and the gaps and challenges that remain in SMFC development that we start to tackle in this paper (see Section 2).
- (2) **Iterative Design for Robustness:** We detail our iterative design process with nine months of combined deployment data to develop usable, computing-centric SMFCs more robust to soil moisture variations. We empirically explore the impact of soil moisture on SMFC performance and present an improved SMFC design that can operate at lower moisture levels and produces more energy, which enabled 40% more computing operations for digital systems and 120% longer runtime for analog systems in simulation than the benchmark cell throughout our 161-day experiment (see Sections 3 and 5.1).
- (3) **Experimental and Testing Framework:** We identify a systematic method to improve the SMFC design by analyzing the performance of its individual electrodes, explaining common experimental pitfalls, and presenting a direct comparison of different cell geometries in lab settings to develop a working prototype as a soil-powered energy source (see Section 4).
- (4) **Real-World Evaluations and Potential Applications:** We contextualize the improvements from our new design with a runtime simulation, evaluate the SMFC under field conditions, and novelly integrate the new SMFC prototype with ultra-low power analog backscatter sensors [11] to gauge the feasibility of soil-powered sensing systems (see Section 5).
- (5) **Community Enablement:** Finally, we release the mechanical designs for our finalized SMFC cell, building tutorials (see Appendix A.2), and simulation tools all online and open source¹ to jump-start research into soil-powered computing.

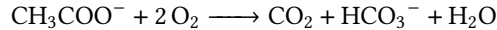
¹We release all mechanical designs and simulation tools at https://github.com/ka-moamoa/Practical_SMFC_Design_Guide.

2 BACKGROUND AND RELATED WORK

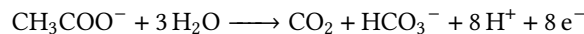
It is only recently that computers have entered the power envelope where the amount of energy we generate in MFCs (hundreds of microwatts) is enough to power practical applications. The rise of low-power Internet of Things (IoT) technologies and distributed sensor networks has sparked an increasing demand for decentralized and renewable – if limited – sources of energy. Despite their promise, most MFC designs are not optimized to produce stable power under dynamic environments with variable moisture contents, which is where these low-power sensors would typically be deployed (e.g., farms, wetlands, etc.). Because MFCs produce power on the microwatt scale, there is also a need to re-examine the fundamentals of current computing and communication methods in order to leverage this ultra-low energy budget. This section explains the theory behind MFCs' operation and the key factors that affect their performance, outlines the knowledge gaps from prior arts, examines the unique benefits of SMFCs as energy sources, and establishes current limitations of soil-powered computational systems.

2.1 Microbial Fuel Cell (MFC) Theory

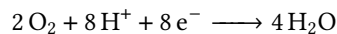
The key components of an MFC are the **anode**, **cathode**, and the **electrolyte** between these electrodes. [Figure 2](#) shows a diagram of the typical soil-based MFC. These cells operate similar to a battery, except they produce power using the organic carbons from the environment instead of depleting the reactants within. In an MFC, organic matter is oxidized by exoelectrogens, which are bacteria that can transfer electrons extracellularly. They are found ubiquitously in most wastewater and soil [96, 99]. The extracellular electrons are then released to a solid-state anode, and travel through a circuit to the cathode, where they reduce O_2 into H_2O while consuming a H^+ in the cathodic half reaction [80]. This process results in a potential difference between the anode and cathode, leading to a source of electrical power. This cell potential equals the difference between the two half-reaction potentials. Using acetate as a simplified representation of the organic growth substrate oxidized at the anode, the overall reaction for the MFC can be written out as:



This can be further broken down into two half-reactions happening at the electrodes. The oxidation half-reaction on the anode side is:



On the cathode, the reduction half-reaction is represented as:



2.1.1 Anode. The SMFC anode can be made from almost any conductive material microbes can grow on. Carbon felt is a popular choice because of its high specific surface area, affordability, low environmental impact, and inert properties [52, 100]. The performance of SMFCs is directly related to the health and activity of the exoelectrogenic biofilm on the anode. Exoelectrogens grow best under anoxic conditions (e.g., in the absence of oxygen), which means that the anode is usually kept away from the atmosphere in MFC designs [98].

2.1.2 Cathode. The cathode can likewise be made from the most inert, conductive materials. MFC cathodes can consist of anything from carbon and metal-based materials to biocatalysts, though biological activity is not necessary for the cathodic reaction to occur [78]. The cathodic reaction is typically what determines the MFC's power output and energy efficiency as it is where the largest over-potential, a factor that decreases harvestable potential, occurs [80]. SMFCs use air (O_2) as the terminal electron acceptor [80], so the cathode often composes of a gas-permeable material to allow for oxygen flow (see [Figure 2](#)).

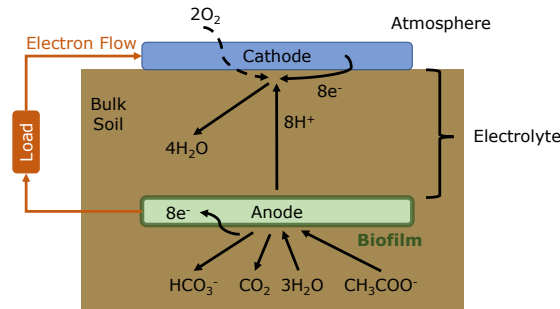


Fig. 2. Basic diagram of a SMFC depicting its anode, cathode, and electrolyte. In a SMFC, the biofilm growing on the anode oxidizes organic matter to release electrons, which becomes the source of electrical power. The cathode performs a reduction reaction to balance out the cell's net charge, which requires oxygen as a reactant. The electrolyte facilitates ion exchange between the anode and cathode while preventing oxygen from penetrating into the anode [80].

Table 1. Summary of the effects of several environmental factors on SMFC power output.

Environmental Factors	Correlation With Power Output	Note
Temperature	+	Power begins to decrease above an upper limit
Organic Matter Content	+	
Soil pH	-	Not always a clear relationship in practice
Soil Moisture Content	+	Sharp drop off after a minimum threshold

2.1.3 Electrolyte. Ensuring the cathode's access to oxygen while maintaining an anoxic anode environment requires an electrolyte between the anode and cathode. SMFCs use a layer of soil as the electrolyte. This electrolyte has to accomplish three tasks: (1) prevent oxygen from penetrating to the anode, (2) insulate the electrodes from one another, and (3) allow ions to diffuse between the electrodes. Without transporting the protons away, the area surrounding the anode will become acidic, negatively affecting the health of the exoelectrogens in the biofilm [76]. An ion exchange membrane can perform the aforementioned functions in an MFC, but the capital cost can be substantial [81]. In SMFCs, oxygen is consumed by aerobic microbes to create an anoxic condition in a deep layer of soil, while the porous structure of the soil matrix allows for ion exchange and prevents shorting between anode and cathode. Whether or not shorting occurs depends heavily on the conductivity of the electrolyte and the separation distance between the electrodes [53].

2.1.4 Key Environmental Parameters for SMFC Performance. SMFC performance is a function of various factors like temperature, soil organic matter content, pH, and soil moisture [92, 101]. The exact model of how any of these parameters affect SMFCs is largely unknown, as even the full diversity of exoelectrogens that SMFCs harness is uncharacterized. Each type of microbe may follow a different metabolic pathway, which currently limits the prediction of SMFC performance using these factors to just general trends [95]. Because the anodic reaction is dependent on microbial activity, increasing the surrounding soil temperature tends to increase the power output of SMFCs, but only up to a certain point (about 36°C according to Zhang et al.) [101]. Since organic carbons species serve as an essential reactant for the anodic reaction, the presence of soil organic matter can also boost the performance of SMFCs [32]. Many groups of exoelectrogens prefer a slightly acidic pH, though it is not well-understood whether a lower soil pH always leads to a higher peak voltage and charge due to the complex nature of soil chemistry [45].

Furthermore, there appears to be a minimum soil moisture content that SMFCs require before sharply declining in energy output (about 20% water by weight in Zhang et al.), which is a significant limiting factor in terrestrial applications where the soil is not saturated [101]. The soil between the electrodes serves as the electrolyte for SMFCs, so desaturating the soil will cause the liquid phase within the soil pore network to discontinue, drastically reducing ion transport and electricity generation [21]. The SMFCs characterized by Chen et al. using soil as the electrolyte experienced a steep drop-off in open circuit voltage with 50% volumetric water content (VWC) [21]. Even SMFCs that use special membranes instead of soil as the electrolyte reported similar results of high soil moisture sensitivity below 48% VWC, making them not viable in many applications [66]. As such, designing SMFCs that are more robust to lower VWC is a highly-motivating yet difficult challenge that we begin to address in this work. The general effects of these environmental parameters on SMFCs can be summarized in Table 1.

2.2 State of the Art of SMFCs

Although several papers have been published on using MFCs as power sources, they have mainly been done with purely aqueous or sediment MFCs in wastewater or marine settings, which are quite different from terrestrial environments [31, 33]. Until recent early-stage work [49, 58], studies geared toward agricultural applications have been limited to crops that prefer inundated environments like rice [51, 90]. Existing papers have demonstrated a strong relationship between soil moisture content and the power output of SMFCs [54, 91], but none has attempted to reduce the power drop caused by decreasing soil moisture to optimize for robust energy production. Some works have implemented strategies like changing the spacing between the electrodes, using different materials for the anode and cathode, and dosing catalysts and nutrient supplements to the cells [87, 100] to improve their relative power output, but only under constant soil moisture. There is a clear need to improve SMFC design for power generation in drier terrestrial environments to bring them into practical use.

A key bottleneck in designing better SMFCs in the existing literature is the lack of robust comparative studies. The design works outlined above (and others [10, 66, 67, 92]) do not perform direct comparisons on how they improve from standard configurations or even explain how they arrive at their prototype. Apollon et al. somewhat explored the effects of soil moisture on the power output of SMFCs in terrestrial environments with their novel SMFC that generates electricity in semi-arid soil [10]. However, their comparison between their cell and those from the existing literature involved many uncontrolled variables, such as soil type, moisture content, temperature, and the microbial communities that generate power in these experiments. Because the power output of SMFCs depends on all of these environmental factors, it would not be fair to evaluate the relative performances of different designs based solely on power production when other variables are not held constant. For example, while the SMFCs from one work achieved a maximum power density of 108 mW/m² [21], this does not necessarily mean they are better at energy production than another that only produced 28.6 mW/m² [45]. The testing conditions between these studies were vastly different, making generalizing performance from comparing these bespoke experiments impossible. **This makes it difficult for SMFC researchers to build on top of each other's work and even harder for the computing community to determine the best SMFC for their application.**

2.3 SMFC as an Energy Source

SMFCs contain comparable energy density to thermoelectric generators (TEGs) and some piezoelectric devices, but orders of magnitude less power than silicon solar cells (see Table 2). However, SMFCs can provide key advantages over existing energy sources from both sustainability and practical standpoints. Their relatively harmless source materials mean they are less likely to threaten their environment. SMFCs do not contain any component classified by the U.S. Environmental Protection Agency (EPA) or Department of Transportation (DOT) as possibly dangerous, which makes them safer for at-scale deployments in protected ecosystems and farmlands.

Table 2. Comparison of various ambient energy harvesting sources showing hazard classifications due to e-waste and toxicity as well as the minerals required to manufacture them. SMFCs are appealing as a ubiquitous energy source due to their low toxicity and hazards, minimally impactful core materials, and competitive performance relative to piezoelectric and TEG.

Energy Source	Performance	Hazardous Classification	Core Materials + Extraction Source
Solar cell	100 $\mu\text{W}/\text{cm}^2$ [73] in illuminated office	EPA: Hazardous [4]	Tin, Silver, Silicon [1, 15, 38, 41] (Open/underground mine)
TEG	0.233 $\mu\text{W}/\text{cm}^2$ [40] average	DOT: Poison [69] (Bi_2Te_3)	Bismuth, Tellurium [29, 42, 65] (Mining byproduct)
Piezoelectric	2400 $\mu\text{W}/\text{cm}^3$ [104] 3 m/s airflow	EPA: E-waste [3]	Quartz, Lead, Zirconium [8, 27, 82, 102] (Open/underground mine, mining byproduct)
SMFC	1.74 $\mu\text{W}/\text{cm}^2$ (see Section 3)	No known hazards	Carbon fiber [62] (Petroleum/biomass)
LiCoO ₂ battery	1363 mAh/cm ³ [68] theoretical capacity	EPA: Hazardous [39]	Lithium, Cobalt [34, 74, 94] (Salt-flat brine, open/underground mine)

Furthermore, the expansion of IoT into increasingly diverse applications has created a need for alternative ambient harvesting sources. For example, farmers or scientists interested in monitoring the soil conditions near certain canopy-dense plants cannot always afford to erect solar panels on tall platforms above the plants for fear of disrupting the plants' growth. In contrast, SMFCs require no ambient light and can be installed underground to avoid unwanted attention. While TEGs can also work under similar conditions by harvesting from the small thermal differential between soil and air, many designs [40] feature heat exchange pipes upwards of 3.5 meters long, which makes their installation laborious and disruptive to the environment.

2.4 Soil-Powered Computational Systems

Prior computational systems that use SMFCs as energy sources use highly controlled (i.e., wet) environments to increase energy output, and a common dilemma they face is the trade-off between functionality, performance, and runtime. For example, basic e-ink displays powered by an array of SMFCs may manage to operate for longer periods, but their capabilities are restricted to simple timekeeping and display [10, 60]. More sophisticated systems only transmit about three data points every two hours due to high power demand [31], and other MFC-powered systems showed similar trends despite leveraging ultra-low power microcontrollers like MSP430 [12, 24, 70, 83].

Even wireless protocols like Zigbee and LoRa, which are specifically designed for low-power applications, struggle to meet the meager energy budget typical SMFCs provide. The MRF24J40MA Zigbee transceiver benchmarked by Pietrelli et al. draws up to 23.3 mA during transmission, which is many orders of magnitude larger than the 557 μA their SMFC generated [75]. Likewise, LoRa-based systems could only achieve a maximum of five transmissions per day despite being connected to an array of three SMFCs [70]. This limits these devices' ability to provide real-time data, which may be critical for implementing the flood sensing application mentioned in Section 5.3.4. Although advances in digital electronics made it possible to intermittently power small devices using SMFCs, microcontrollers and radio transmitters are still very costly to implement energy-wise.

Josephson et al. pointed out the possibility of using RF backscatter to transmit sensor data in SMFC-powered systems, which we build upon in this work [49]. Backscatter operates on the order of nanowatts, making them suitable for SMFC-powered applications [72]. Through the use of a purely analog backscatter device like MARS [11], we expect near-continuous runtime with just the power from a single SMFC assuming it is not dried out. Analog backscatter devices offer unmatched performance in terms of runtime availability and robustness without using batteries and storage capacitors, making them a more viable choice for the real world. An in-depth assessment of integrating MARS with SMFC is explored in Section 5.

3 SMFC DESIGN ITERATION

While the theory of SMFCs is fairly simple, the challenge of implementing a robust working cell has impeded research into soil-powered computing. Previous studies have tried to use low-performance, basic cells (see Figure 2) that were originally designed for contaminant removal [92] and had to maintain inundated environments to achieve high power output [51, 90]. The works that have proposed different SMFCs rarely examine their relative strengths and weaknesses and never explain their design rationales [10, 66, 67, 92]. This has made SMFC a difficult subject for non-experts to explore. We describe our three design goals and the challenges we must overcome to enable soil-powered computing as a field below:

Design Goal #1, Robustness: Improve the SMFC’s power output continuity by increasing its robustness to soil moisture variations. This is difficult due to the soil electrolyte’s dependence on water for ion transport. Extending the moisture range at which SMFCs can operate will make them more stable power sources, which is vital to implementing reliable SMFC-powered sensors.

Design Goal #2, Reproducible and Understandable: Establish a framework for experimental procedures to streamline the process of testing different SMFC designs. Standardizing SMFC experiments is challenging because of the number of variables involved that affect their performance (specific soil used, electrode alignment, temperature, etc.). Having a well-tested experimental setup with examples of common pitfalls and how to debug them will make the complex nature of SMFC design involving wet lab work, electronics prototyping, and living organisms more accessible to the computing community.

Design Goal #3, Accessible and Local Supply Chains: Provide easily manufacturable baseline SMFCs for future work. Most SMFCs in literature are not well-characterized in terms of construction and performance under dynamic conditions. As such, creating easily-reproducible SMFCs with purely off-the-shelf and 3D-printable components that have also been tested under a variety of moisture conditions will enable researchers to compare their own designs with these as benchmarks.

Toward these goals, we detail our 2-year-long iterative design process of prototyping and data collection to improve the robustness of SMFCs by altering their electrode geometry. We begin with a preliminary study to characterize common issues with traditional SMFC designs (Section 3.2). We then describe a series of iterations (Sections 3.3, 3.4, and 3.5) where we modified the geometry of the SMFCs to optimize their computationally usable energy output for lower moisture environments. The SMFC designs explored features the following:

- v0:** Horizontal anodes and cathodes (**control**)
- v1:** Vertical cathodes with vertical anodes
- v2:** Vertical cathodes with horizontal anodes
- v3:** Horizontal anodes with one side of the vertical cathodes permanently exposed to air

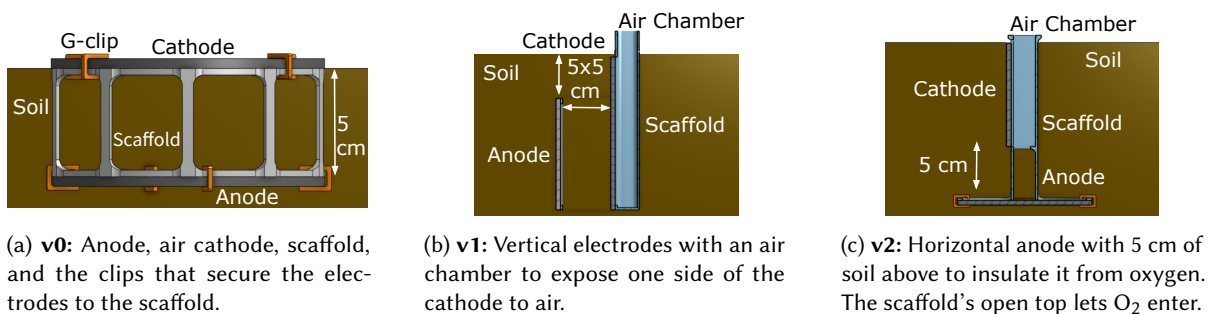


Fig. 3. First three iterations of the SMFC that led to the improved v3 design.

The first three versions of our SMFC (see [Figure 3](#)) served as vital benchmarks to point out shortcomings in our concepts, which led to our final v3 prototype. Our iterative design work on SMFC distinguishes itself by focusing on directly comparing the performance of SMFCs with different electrode geometries against each other given identical environmental factors. This serves as a more practical guide toward designing soil-powered energy sources for *computing* in remote terrestrial environments.

3.1 Experimental Setup

All of the following experiments were carried out in a lab at room temperature ($20 \pm 1.5^\circ\text{C}$). A Raspberry Pi 3B along with 16-bit ADS1115 analog to digital converters were used to record the median voltage values of each cell every minute. To avoid any confounding of electrochemical corrosion [47], titanium wires (Ultra-Corrosion-Resistant Grade 2 Titanium Wire 0.025" Diameter) insulated with polyolefin heat shrinks (Digi-Key Q2F364B-100-ND) were used to connect the electrodes of the SMFCs to external electronics. The titanium wires were used for experimental evaluations only and can be replaced with carbon-based conductors for real deployments. The electrodes were made from 4.5 mm carbon felt (G600 AvCarb Soft Graphite Felt) based on prior work [87]. A 2 k Ω resistor connected the anode and cathode of each SMFC. This load was chosen to maximize the power produced by the cell as determined by Lin et al. [54]. The soil used for these experiments was collected from the university's graduate student garden (see [Appendix A.1](#)), which we air-dried and sieved through a 2 mm mesh to remove large particles such as gravel, rocks, and any plants and insects. Before the SMFCs were installed, deionized water was added to the soil to reach the target soil water content, and the mixture was thoroughly stirred until it became a homogeneous slurry. Duplicates were operated for the experiment in [Section 3.2](#), while triplicates were operated for [Sections 3.4](#) and [3.5](#). All of the cells featured a constant 5 cm anode-cathode separation with a base surface area of 126.7 cm² per electrode unless otherwise mentioned, which prevents the electrodes from shorting and ensures sufficient surface area for exoelectrogens to colonize [6]. During the startup periods of the experiments, the soil was kept flooded with the top of the bulk container partially closed to slow the rate of evaporation. A step-by-step instruction for how we set up these comparison experiments and built the cells described in this section can be found in [Appendix A.2](#).

3.2 v0: Control Setup with Horizontal Anode + Horizontal Cathode

In order to better understand and improve upon the weaknesses of traditional SMFCs (see [Figure 2](#)), we first benchmarked a design inspired by the Mudwatt, a commercial SMFC from Magic Microbes [6]. In our experiment, two identical carbon felt disks with a diameter of 12.7 cm were used as the anodes and cathodes of the SMFCs. The cathodes (top carbon felt disk) were kept exposed to the air while the anodes (bottom carbon felt disk) were buried in the soil under anoxic conditions (see [Figure 3a](#)). A TEROS-12 sensor from METER was used to monitor the bulk volumetric water content (VWC) of the setup.

3.2.1 Results. Over the course of this experiment, Cell 2 produced upwards of 222 μW with a power density of 1.74 μW per cm² of geometric cathode surface area at its peak. Power density is normalized to cathode surface area because the cathode is usually the limiting factor in MFCs (see [Section 2.1.2](#)). [Figure 4](#) shows that even though the bulk VWC of the setup was held relatively constant, there was a sharp decrease in power production around day 10 of the experiment. It was observed that the top 1 cm of the soil dried up around that time, leaving the cathode cut off from the water-saturated portion of the environment. It is likely that this regional decrease in soil moisture content disrupted the ion transport in the electrolyte described in [Section 2.1.3](#), thus breaking the reaction necessary to generate electricity. As such, a series of design iterations was performed to explore three new SMFC prototypes with different anode and cathode orientations to address this issue. In the subsequent experiments, this v0 cell with horizontal anode and cathode served as the control for the new designs. 3D-printed scaffolds made of plant-based PLA plastic were added to the design to aid with their installation (see [Figure 3a](#)).

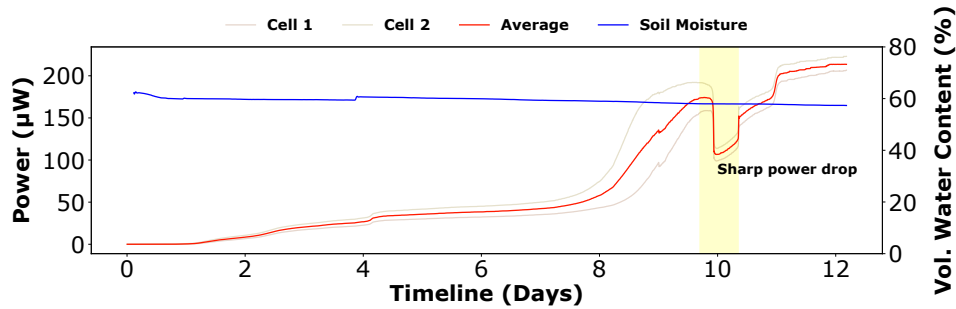


Fig. 4. v0 control study data demonstrating the sharp drop in power despite no obvious change in bulk volumetric water content, suggesting that the regional decrease in soil moisture affected the cells' power outputs.

3.3 v1: Reduce Electrode Drying with Vertical Anode + Vertical Cathode

3.3.1 Challenge. The v0 cell power outputs drastically decreased after the top layer of soil dried out. This reduced the output power to zero despite an abundance of moisture in the environment. As such, our design must **prevent the electrolyte from drying out** and cutting off ion exchange between the electrodes.

3.3.2 Solution. In order to prevent the sudden cutoff in power after the top layer of soil dries, we decided to **rotate both electrodes so that they lie perpendicular to the soil surface** (see Figure 3b). This means that as water evaporates from the soil, both electrodes would still sit partially in the water-saturated region, theoretically allowing ion transport to happen as long as the cell was not completely dried out. One side of the cathode is kept in contact with soil, while the other side is exposed to air using an air chamber formed by the PLA scaffold. The surface area of the anode was kept the same as the anodes in Section 3.2, while the cathode was made slightly larger to allow it to extend closer to the soil line. One cell was kept under inundated conditions in the lab to test the viability of this design.

3.3.3 Results. As one can see in Figure 5, the v1 cell performed far less reliably than the v0 cells benchmarked earlier. Even though it was kept in the same type of soil as the cells in Section 3.2, it never established a consistent power output, and the voltage readings between the electrode did not indicate the steady microbial growth that typical SMFCs have.

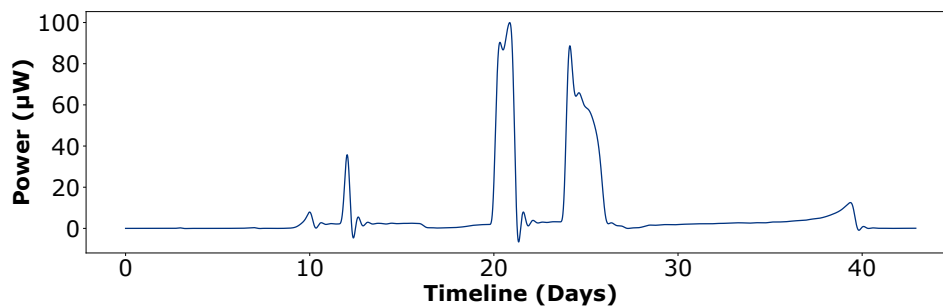


Fig. 5. v1 cell performance showing no clear microbial activity after 40 days of incubation due to the possible infiltration of oxygen to the anode. This iteration is insightful for determining the best configuration for the anode, which we implemented in the v2 SMFC prototype (see Section 3.4.2).

In order to debug this issue, we measured the potential of both the cathode and anode relative to an AgCl electrode (BASi MF-2052) placed very close to the electrode in question [63]. It was found on day 20 of the experiment that the cathode to reference potential was 311.7 mV while the anode to reference potential was 216.3 mV. Since the anode potential was relatively high (indicating a lack of oxidation reaction happening), we hypothesized that flipping the anode vertically had a negative effect on its performance, and adjusted that for the next design. One possible explanation for this reduced anode performance is that the vertical anode may contain less surface area in an anoxic environment, limiting exoelectrogenic activity.

3.4 v2: Prevent Oxygen at Anode with Horizontal Anode + Vertical Cathode

3.4.1 Challenge. The **anode performance of v1 cells was poor**, and the overall cell output was very inconsistent despite constant environmental parameters. The vertical arrangement of both electrodes might have somehow encouraged the formation of small cracks in the soil that transported oxygen to the anode.

3.4.2 Solution. This new SMFC iteration utilizes a **horizontal disk** identical to the v0 electrodes for its **anode** and a rectangular carbon felt **perpendicular to the anode** and equal in surface area as its **cathode** (see Figure 3c). One side of the cathode is kept in contact with soil, while the other side is exposed to air using an air chamber formed by the PLA scaffold. All of the v0 control cells and v2 cells were placed within the same bulk container (6 cells total) and flooded until the water level sat just below the control cells' cathodes. The container was then covered with a plastic tarp until all of the cells reached steady state. After that, the tarp was removed to allow water to evaporate in order to characterize the SMFCs' behaviors across a range of soil moisture values. We performed the moisture cycle twice to observe how different cell types rebound from drying.

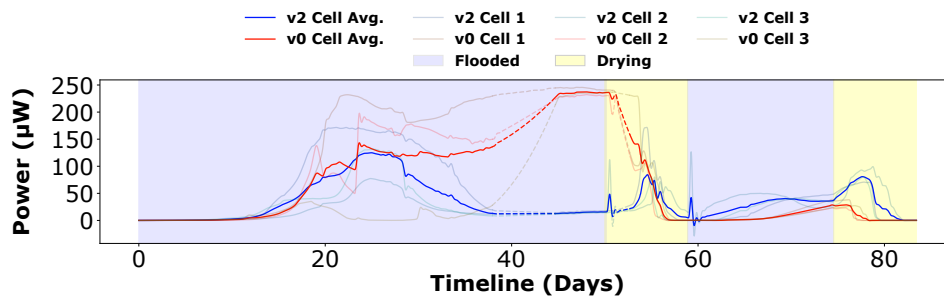


Fig. 6. v2 cells vs. v0 cells across two moisture cycles. Cycle 1 is from day 0 to day 52, and Cycle 2 is from day 53 onward. The v2 cells showed increasing power during drying cycles and recovered better from drought, demonstrating the promise of altering to a vertical cathode geometry. However, the vertical v2 cathodes being completely submerged during flooded periods caused their performance to suffer, which we address through our v3 prototype in Section 3.5.2.

3.4.3 Results. During the initial startup phase, the v2 cells seemed to follow a similar trend to the controls. However, their powers steadily declined after day 32 of being kept in flooded conditions, while the controls maintained their output for the most part (see Figure 6). In the first drying period, all of the control cells' outputs dropped steeply to almost zero. The v2 cells, on the other hand, experienced a boost in power before declining with their neighbors. This same pattern can be seen in the second drying cycle, and the v2 cells also seemed to recover faster than the controls after being dried out, although all 6 cells had the highest power outputs during the initial flooded period. The relatively linear trends from days 38-45 and 50-53, represented by dashed lines, are extrapolated due to data loss from a logger malfunction.

Throughout the experiment, the air chambers of the v2 cells were flooded with water, making the air cathodes partially underwater. This was especially apparent during the flooded part of the moisture cycles, where the air cathodes were entirely submerged at times. Because the cathodic reaction requires oxygen, partially submerging the cathode would reduce its effective surface area and the cell's power output. While oxygen could still diffuse into the water in the air chamber from its surface, it would quickly be used up by the aerobes breaking down the soil underneath in an established system, which could explain the delayed drop in power for almost 33 days. During the first flooding period (day 36), v2 Cell 2 had anode and cathode potentials of -463.3 mV and -338.8 mV respectively relative to a AgCl reference electrode, while v0 Cell 2 had anode and cathode potentials of -435.7 mV and 92.1 mV respectively. This further suggests that the issue lies with the cathode, as the two cells' anode potentials were relatively the same while the v2 cell's cathode had a much lower potential. Although the v2 cells did worse than the controls when the enclosure was flooded, they achieved better theoretical runtime than the v0 cells during both drying periods and the second flooded period. This indicates that a vertical cathode geometry allowed the cells to function at more dynamic moisture conditions. In order to take advantage of this added robustness from the vertical cathode design while also maintaining steady performance in flooded soil, the air chamber was sealed from the environment for the next iteration.

3.5 v3: Provide Oxygen to Cathode with Sealed Air Chamber Design

3.5.1 Challenge. In the v2 cells, water was able to infiltrate the air chamber through the bottom of the scaffold and the porous cathode itself (see [Figure 3c](#)). The air cathodes get **submerged in water during flooded periods**, which limits the cathode's access to oxygen, consequently reducing the cathodic reaction rate.

3.5.2 Solution. We ensured the air cathode's access to oxygen in this iteration by extending the 3D printed scaffold to enclose the bottom of the chamber, thereby **sealing the air chamber from the soil environment**. This scaffold was printed using ABS on a Stratus Fortus 250mc to enable the use of water-soluble support structures so that we can accommodate the large overhang from the window cutout in the front of the scaffold. We also constructed a waterproof cathode using a combination of 30% wetproofed carbon cloth from Fuel Cell Store, carbon felt, room-temperature-vulcanizing silicone, and a custom 316 stainless steel flange so water could not enter the chamber through its side (see [Figure 7](#)). The screws (McMaster-Carr 90666A131) and nuts (McMaster-Carr 93935A335) used were made of 316 stainless steel, as well. Three replicates of these v3 cells were placed side by side with three v0 control cells identical to the setup described in [Section 3.4](#). A METER ECH2O EC-5 soil moisture sensor was used to log the soil's VWC over time.

3.5.3 Results. v3 cells showed significant improvements over v2 in this experiment (see [Figure 8](#)). This design no longer has the issue of decreasing power output after being submerged for extended periods like v2, and it also kept the enhanced recovery rate that the v2 cells had after being re-hydrated in the second flooded period. v0 Cell 1 was omitted from the average calculation after day 137 (vertical gray dashed line) due to logging disruptions. The v3 cells outperformed the control cells throughout the entire experiment except for part of the first drying period. This trend of increasing power outputs from v0 during the drying period was most likely a result of experimental error, as it was not seen in [Section 3.4](#) and the following three drying periods in [Figure 8](#). The PLA clips that secured the v0 cathodes to their scaffolds broke around day 28 (vertical green dashed line), which required the cathodes to be pushed down into the soil so they could be reattached to the scaffolds. This improved the cathodes' contact with the wet soil underneath, artificially boosting the electrolyte's ability to transport ions.

Similar to the results from [Section 3.4](#), the first moisture cycle achieved the highest power output, with the subsequent cycles stabilizing to a lower level. This behavior is likely an artifact of our soil preparation process, which includes completely air-drying all of the raw soil so it can be sieved and homogenized prior to installing the SMFCs. Rewetting dry soil can cause a burst in biologically available carbon, which has been observed to correlate

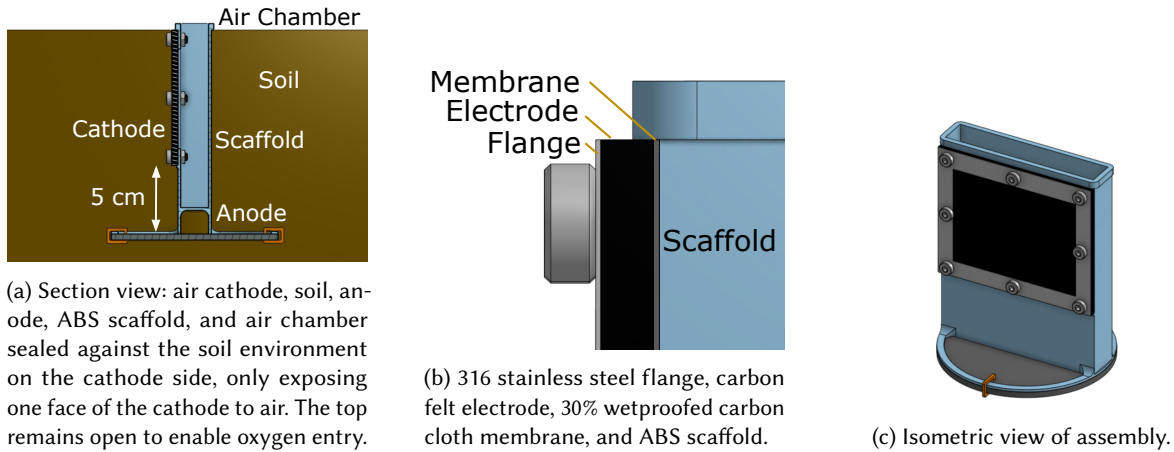


Fig. 7. v3: Sealed air chamber cell design to prevent the cathode from being submerged during flooded periods.

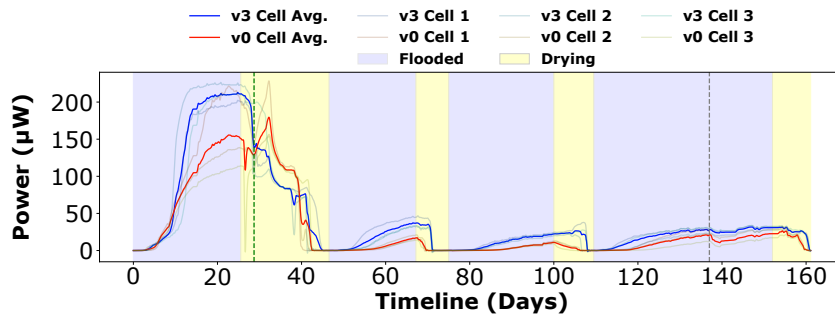


Fig. 8. Power from v3 cells vs. v0 cells across four moisture cycles. The v3 design outperformed the v0 benchmark throughout nearly the entire experiment, featuring better power output during flooded periods and faster recovery from droughts. The SMFCs' power was the highest during the first moisture cycle and remained relatively the same in subsequent cycles (about 30 μ W for v2 cells and 15 μ W for v0 cells).

with a sudden surge in CO_2 production in what is known as the Birch effect [88]. This effect is exacerbated by extreme swings in soil water content and mixing of the soil, both of which were part of our experimental procedure. This, combined with the stable outputs in subsequent moisture cycles, indicates that the initial power decrease doesn't signal SMFCs depleting their organic carbon source. In fact, we saw no appreciable decrease in total organic carbon (TOC) between the soils surrounding the cell anodes and the bulk soil even after months of operation (see Table 6). In natural environments, TOC is replenished by plants and animal activities, which we postulate can offset the minute carbon consumption of SMFCs and keep them operating indefinitely [20]. This suggests that SMFCs can keep producing power given sufficient moisture from the environment.

The relationship between VWC and power can be visualized in Figure 9, where it shows the power discrepancy between the v3 and v0 cells during the second drying period. While the average v0 cell output dropped linearly to 0 μ W between VWC of 46% and 44%, the v3 cell power seemed unaffected by VWC until it decreased down to the 42% mark. This means that v3 cells were more robust to changes in surrounding moisture contents, making them more suitable for power generation purposes. This 4% improvement in functional VWC range, though limited, is significant considering this is the first example of altering SMFC design to improve their robustness

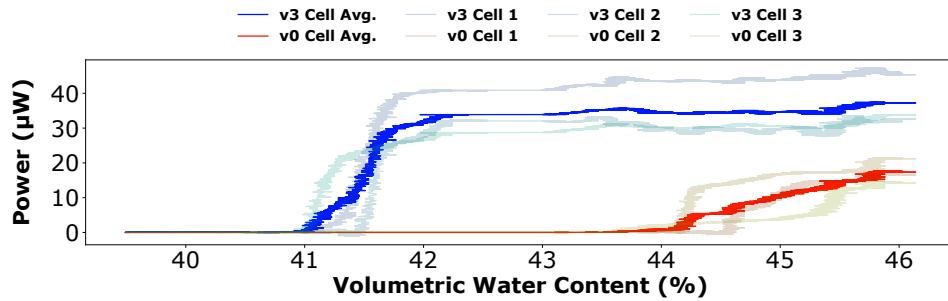


Fig. 9. Power output comparison of v0 and v3 cells as a function of VWC during the second drying period, where the v3 cells were able to perform at a 4% lower VWC, making them more robust to lower soil moisture levels.

to soil moisture content. The high VWC value in the experiment ($>40\%$) likely means that even the v3 SMFCs would not do well in the comparatively drier agricultural soils [26]. However, many grasslands and marshes have soil moisture levels hovering around 40-50% [25], making lowering the minimum VWC requirement for SMFCs in this range critical for many environmental monitoring applications. It is interesting to note the steep slope of v3 cells' power decline. This aligns with prior work that hypothesized how air invasion in the electrolyte soil layer leads to the discontinuity of its liquid phase, hindering the ion transport between the electrodes and stopping power production abruptly [21]. This suggests that future efforts with SMFC iteration should explore re-designing the electrolyte so that its ion exchange capability can be independent of its moisture content. The implications of v3 cells' increased functional VWC range on computing is further explored in Section 5.1.

Although the v3 cells made drastic improvements over previous iterations in terms of power output and robustness, there are still items that should be addressed to improve the practicality of the design. Because the anode of the v3 cell was made identical to the v0 anodes to eliminate variables, the base of the cell ended up being much wider than the top, making insertion into soil difficult. Furthermore, the thin PLA ring that the anode disk gets clipped to is prone to breaking when the cell gets dug out, reducing the reusability of these devices. The material selected for the prototype also did not create a tight enough seal in the cathode air chamber, and water was able to infiltrate in small amounts into Cell 2 and 3's air chambers after 2 months. The water was manually removed with a pipette during the experiment to avoid submerging the cathodes, which would not be feasible for autonomous deployments. In addition to improving the quality of the seal, a real cell deployed outdoors would need to be modified to prevent rain from entering the top while still allowing airflow. These issues were resolved by the use of a thicker, more monolithic scaffold composed of plant-based PLA plastic in Section 5.

3.6 Design Iteration Summary

Our experiments optimized SMFCs' ability to power computing devices by changing the relative orientations of their electrodes. This made the cell more robust to changes in VWC and produce higher power overall, which makes it a more stable power source for low power electronics. The v0-v2 cells had a number of shortcomings that were addressed by their respective successors, which led to the conception of the improved v3 design. A summary of the key design issues and improvements can be seen in Table 3. While this work took the first steps in building more robust SMFCs by manipulating cell geometry to improve their performance, further iterations will be needed to optimize SMFCs for real-world applications, such as adopting a solid-state electrolyte that performs independently of moisture content and adjusting the form of the cell to integrate the electronic components necessary for wireless sensing. This section presents the learnings from our exploratory trials, which we contribute as a template for future work on improving SMFC designs.

Table 3. Summary of the design exploration for computing-focused, power-optimized SMFC cells. Testing required a number of weeks per cell version to allow the microbial community to form, stabilize, and react to changes. Through each iteration, we uncovered design requirements and challenges when deploying in terrestrial settings while maintaining sufficient power levels for computing elements. **One side permanently exposed to air*

Version	Improvements	Issues	Anode Orient.	Cathode Orient.
0	-	The power output dropped very steeply after the top 1 cm of soil dried out due to disruptions in the ion exchange process.	Horizontal	Horizontal
1	Performed worse than v0 cells	Cell output was very inconsistent with abrupt power spikes, indicating little microbial activity during most of its operation.	Vertical	Vertical
2	Better performance during drying periods and recovers faster after re-flooding cells.	Power level gradually decreased after being inundated for about a month.	Horizontal	Vertical
3	Maintained significantly higher power throughout flooded periods; operated with 4% less VWC.	Difficult to install and extract, and minor leaks in this air chamber design must be fixed for long-term and autonomous deployments.	Horizontal	Vertical*

4 LESSONS LEARNED

From the data and observations gathered throughout the design iteration process described in Section 3, we extracted a debugging framework to systematically test and improve SMFC performance. We also compiled a list of common issues in setting up SMFC experiments and how to address them. Our framework uses reference electrodes and external sensors to identify whether the bottleneck to achieving higher power lies in the anode or cathode of the SMFC. This method evaluates cells based on their relative performances and can serve as a powerful tool for future researchers to optimize SMFCs for their desired purpose. Since each SMFC experiment can take months to conduct, sharing our methods and learnings will help future SMFC researchers shorten their design cycles and accelerate the field of soil-powered computing as a whole.

4.1 Debugging Framework

Because there are so many factors that could affect the performance of SMFCs (see Section 2.1), we have found it to be imperative to **compartmentalize cell designs into modules that can be improved individually**. One of the most effective tools we used to identify issues in our cells is the reference electrode. In existing studies on the behaviors of aqueous MFCs, there are 3-electrode cell architectures featuring a working electrode (the biotic anode), counter electrode (the abiotic cathode), and an additional reference electrode (typically AgCl) [103]. Although this configuration is typically used with a potentiostat to perform advanced analyses like cyclic voltammetry [61], we instead leveraged it to evaluate the SMFC's anode and cathode potentials separately (see Figure 10). As Section 2.1 stated, the total output voltage from a SMFC is the difference between the potentials from the anode and cathode half-reactions. Therefore having insights into which half-reaction is underperforming will allow us to make specific changes that target the electrode in question.

Once we understood which electrode performance is the limiting factor, we were able to make more informed decisions regarding sensor selection and experimental design to identify precisely why that electrode was behaving poorly. For example, in Section 3.4.3 we observe that E^+ was poor while E^- looks normal, so we did not invest resources into sampling the biofilms in the soil or install an oxygen sensor to monitor O_2 penetration into the soil since neither of those affects the cathode performance. A significant challenge in this methodology, however, is determining what a "poor" E^+ or E^- actually is. Although the theoretical standard potentials of the

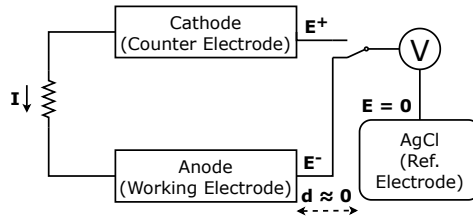


Fig. 10. Schematic of the 3-electrode SMFC configuration to measure anode and cathode potentials relative to the reference electrode (E^- and E^+ respectively). The reference electrode should be placed as close as possible to the electrode one is measuring to avoid uncompensated ohmic drop, which can skew the voltage measurement [103].

anode and cathode half reactions are known to be -0.29 V and 0.81 V relative to a standard H_2 electrode (SHE) respectively [80] (or -0.49 V and 0.61 V relative to a AgCl electrode because the AgCl electrode potential relative to SHE is 0.197 V [2]), these numbers are calculated using just acetate as the substrate and do not take into account the vast diversity in the types of organic carbons exoelectrogens oxidize in the soil. A number of other external factors described in Section 2.1.4 make comparing measured E^- and E^+ to an absolute standard impractical since the measured values will always deviate from their theoretical counterpart just due to effects from these environmental conditions.

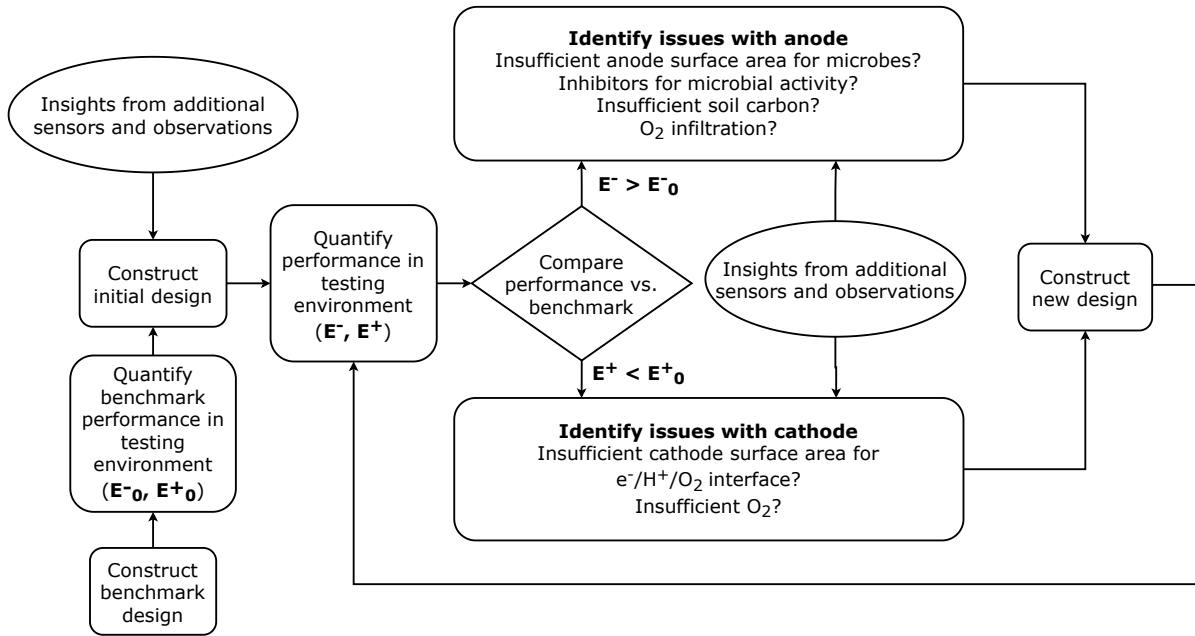


Fig. 11. Flowchart outlining the iterative design process featuring a relative benchmark that new designs are tested against in the same environment.

As such, we found the better approach to be comparing the measured E^- and E^+ values of a designed cell to their corresponding values from a benchmark cell in the same environment. These relative comparisons can then be used with additional sensor data (temperature, moisture, pH, O_2 , etc.) and insights from SMFC theory

to identify issues in the design and improve upon them. Our suggested framework for identifying weaknesses in SMFC design and iteratively improving them can be seen in Figure 11. Examples of where we used this reference electrode method can be found in Sections 3.3 and 3.4, where we evaluated the measured potentials to identify issues in anode and cathode performances respectively. We selected a Mudwatt-based design (v0) as the initial benchmark due to its widespread use in existing literature and simple construction. We periodically spot-checked electrode potentials using AgCl reference electrodes instead of permanently burying them for continuous measurements since they are ruined easily by membrane fouling and drying in soil. Using reference electrode readings combined with a VWC sensor and visual observations lets us systematically identify design bottlenecks and target our approach on the two electrodes accordingly. This framework can speed up SMFC's design process, which is vital to developing soil-powered ubiquitous computing.

4.2 Common Issues and Solutions in SMFC Experiments

To inform future researchers of potential pitfalls in SMFC experiments, we listed some of the common issues and their respective solutions from our 2-year-long prototyping and design iteration experience below:

4.2.1 Large variability in cell performance. Prior to setting up the v0 experiments in Section 3.2, we have experienced large variations in the behaviors of different cells due to local differences in soil texture caused by the presence of rocks and branches. This can make experiments very difficult to replicate and result in theoretically identical cells producing vastly different outputs in the same environment (see Figure 12). To resolve this, we thoroughly sieved the raw soil used for all of our experiments so they are all within the same range of soil texture and particle size. We also wetted the soil into a slurry and mixed it extensively to make it more homogenous prior to embedding the SMFC, since dry soil will naturally separate out by particle size due to granular convection, causing variations in soil texture at different depths [56].

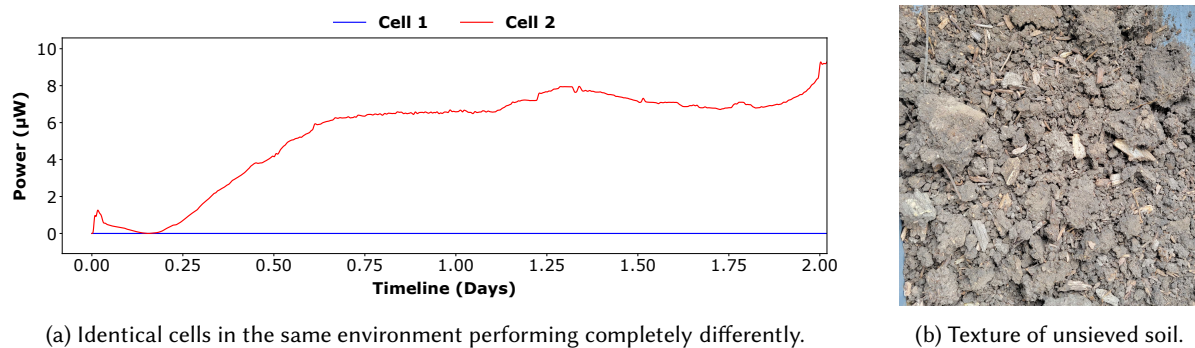
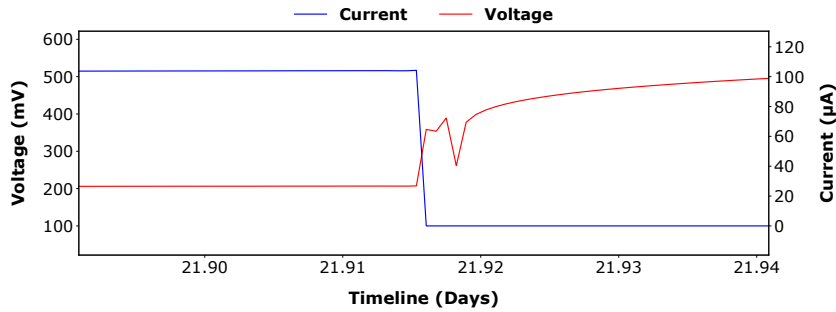


Fig. 12. Soil texture variation can vastly affect cell performance, making it critical to sieve soils for reproducible experiments.

4.2.2 SMFC voltage quickly dropping. Because SMFCs are buried in soil, mud and water may get between the carbon felt electrode and the wire connecting it to the external circuit. As such, if the wire is not properly secured to the felt, the connection between the wire and the felt may break, sharply reducing the voltage of the SMFC despite no sudden environmental change (see Figure 13). To resolve this, we made sure to weave at least 3 inches of clean titanium wire into the felt prior to burying the cells, and installed external strain relief to avoid accidentally ripping out wires from their respective electrodes. We also probed the exposed end of each wire and the far side of its corresponding electrode using a multimeter to test for continuity prior to burying our cells.



(a) Sharp drop in current coupled with increasing voltage in a SMFC.



(b) Dirty/disconnected wire.

Fig. 13. Poor connection between the load circuit and the carbon felt electrode can result in increasing voltage, which throws off the power measurement.

4.2.3 SMFCs not incubating. We have observed instances of SMFCs only going up to 10-20 μW after weeks of incubation despite an abundance of water. This may have a number of causes ranging from low microbial activity or diversity to the soil directly touching the cells not having sufficient organic carbon. While the exact causes are not always known, digging up the cells, thoroughly remixing the soil with a lot of water, then reburying them usually resolves the issue. If doing this a couple of times still does not allow the cells to climb to the $>100 \mu\text{W}$ range while connected to 2 $\text{k}\Omega$ resistors, then one should try re-incubating in a different soil.

4.2.4 Soil VWC measurements not changing. Since SMFCs react to VWC changes on such a local scale (just the top few cm of soil around the cell), it is difficult to correctly capture this change with conventional equipment. Most commercial VWC sensors have relatively large measurement volumes, making them ineffective at capturing the VWC changes that affect SMFC power (see Section 3.2). To ensure that relevant trends in VWC are sufficiently captured in SMFC experiments, one should choose sensors with as small of a measurement volume as possible and install them at the same height in the soil column as the SMFC cathode. One should also eliminate any large particle or air pocket near the sensor if a capacitive VWC sensor is used to avoid lowering its sensitivity.

5 EVALUATION

To further gauge the feasibility of soil-powered sensing systems given the limitations of current SMFCs, we conducted a number of evaluations using the data and prototypes produced from Section 3:

- (1) **Computing Runtime Simulation:** We simulated runtime for different computing modalities using real-world SMFC voltage traces from our design iterations, contextualizing the performance impacts of our redesigned v3 cell with improved energy production.
- (2) **Outdoor Evaluation:** We deployed a modified v3 SMFC (v3.1) in realistic outdoor conditions and analyzed its performances alongside soil moisture data to determine if it can achieve useful power levels in the field.
- (3) **Soil-Powered Backscatter Sensor Demonstrations:** We integrated SMFCs with low-power analog backscatter sensors, known as MARS tags [11], for touch and soil moisture sensing, showcasing the potential of soil-powered wireless sensors.

This section contextualizes the importance of our framework and the design improvements we made from the v0 benchmark cell to the new v3 prototype. We detail the method, results, and conclusions we draw from each of these evaluations, which enables us to assess the implications of SMFCs from a more practical standpoint.

5.1 Computing Runtime Simulation

In this analysis, we simulated the theoretical number of operations one could achieve with our v3 cell design compared to the control v0 cell. We built the simulation using real-world SMFC voltage traces collected throughout our design iterations (161 total days of data collection from Section 3.5) alongside datasheet values for three computing modalities. This simulation serves to demonstrate how much improving SMFC's robustness (even just by a little bit) matters for computing by benchmarking the number of theoretical operations one could execute given different SMFCs' power levels. Specifically, we seek to answer the following questions:

- (Q1) What comparative performance can we expect for SMFC-powered computing across a range of devices?
- (Q2) What is the computing performance impact of our re-designed cell with more stable energy production?

The simulation presented below lets us explore these questions repeatably while relying on actual, real voltage traces collected from our cells. The simulator replays the voltage and current traces of real-world SMFCs, yet it does not model the SMFC itself nor the various environmental parameter's impact on the cell. Instead, this trace-based simulator allows us to compare SMFCs in different environments, or different SMFC designs, merely by capturing a few traces of their output. This is standard operating practice in other work exploring the utility of new energy harvesting sources, including simulators/emulators like Power TOSSIM [84], SIREN [35], GreenCastellia [16], and Fused [97], which all support trace-based emulation in the spirit of our simulator.

This evaluation contributes by comparing performance and operation to better understand how we enable novel computing applications powered by soil. We investigate our SMFCs as power sources for two traditional and one emerging computing paradigms:

Advanced, High-Capability Systems: These are edge devices with more advanced sensing, computing, and communicating tasks. These devices often heavily rely on checkpointing and other intermittent computing elements to accomplish tasks over time [23, 28, 55]. As a representative example, our analysis will consider the LoRa-based system described by Jagtap et al., as such long-range communication capability will likely be important to many SMFC deployment scenarios [44].

Minimal Digital Systems: These are minimalist edge devices that attempt to use as little energy as possible to do something useful. The quintessential example is the "Monjolo"-style sensor, which only boots and sends empty packets; the rate of packet transmission is the sensed signal [18, 30]. As a representative example, we will consider the Cinamin beacon, which solely attempts to send BLE advertisement packets [17].

Analog Systems: An emerging class of novel devices is "computational materials", systems of even-lower power, which save power by omitting digital logic and leveraging passive or semi-passive communication techniques to enable sensing on record-low energy budgets [37, 48, 50, 64]. As a representative example, we will consider the MARS tag: a purely analog, backscatter-enabled, ultra-low power, and inexpensive sensing device [11]. As MARS reported numerous performance specifications, we use this work as a stand-in for the wide variety of analog backscatter-enabled sensing work.

5.1.1 Method. To account for the fact that microcontrollers and peripherals such as the Dialog DA14581 and Murata CMWX1ZZABZ-078 require higher operating voltages and bursts of instantaneous power that exceed the roughly 200 μ W produced by our SMFCs, we assume that all three system types receive energy through a power harvester circuit that charges a storage capacitor from either a single v0 or v3 SMFC cell's output (see Figure 14). This architecture is similar to most battery-free and intermittently powered sensing literature [9, 13, 43]. We set up a simulation environment similar to previous research on predicting the performance of energy harvesting computing, given the highly dynamic and unpredictable nature of energy harvesting in the field. [14, 35, 36, 57, 79].

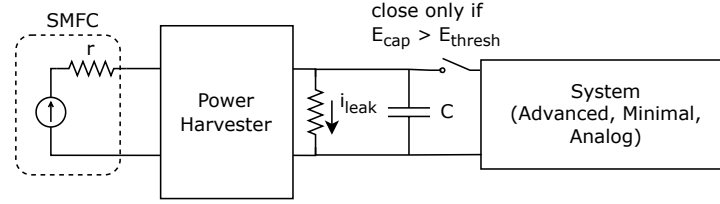


Fig. 14. Schematic of the simulated setup. The SMFC is the *Energy Source*, the harvester, storage capacitor C, and switch are the *Energy Buffer* and *Charge Controller*, while the *Energy Consumer* varies based on the application. We use a fixed *Charge Controller* but explore how the *Energy Buffer* varies with application. In the simulation, the power harvester opens the switch when E_{cap} is below E_{thresh} .

The average voltages across all v0 and v3 cells are similar, so we took the average of all the voltage traces among Section 3.5 and used them to calculate the expected energy accumulated on the storage capacitor.

While numerous circuit models exist for aqueous MFCs, little has been done to model the behavior of *soil*-based MFCs. To date, the best-known model treats the SMFC as a constant current source with complex dynamics under AC loads. These dynamics are ones a cell may be subjected to by a switching boost regulator in a harvester IC [19]. The longitudinal sampling of cells from our experiments subjected the cells to a fixed DC load of 2 k Ω . The measurement setup recorded cell voltage under this load every sixty seconds. An MFC-aware harvester should be able to match or exceed the power extracted from the cell with a static load [58]. Therefore, we assume constant power output from the MFC between each sampling timestep to simplify our modeling.

In the absence of any MFC-optimized harvester ICs, we turn to the Analog ADP5091 instead, which was previously used in SMFC systems [58, 59] and is designed to work with low-voltage sources. It is roughly 60–80% efficient over the range of voltages that SMFCs can generate. In each timestep, we consider the efficiency of regulator at the current SMFC output voltage². η_{ADP} represents the percent efficiency of the ADP5091 harvester given an input power from the SMFC.

We assume no loss charging the capacitor, however, we must account for the leakage of the storage capacitor, as even low-leakage tantalum capacitors common in energy harvesting designs have losses significant to application behavior. Using a KEMET T491 as a reasonable representative measure, we expect the storage capacitor leakage current to be $i_{leak} = 0.01 \times C \times V_{cap} t \mu A$.

Putting all this together, our final model for the energy in the storage capacitor over time (not yet accounting for energy consumed by the system load for the application) at step $n + 1$, or $E_{cap,t_{n+1}}$, is:

$$E_{cap,t_{n+1}} = E_{cap,t_n} + \underbrace{\underbrace{V_{SMFC_n}^2 / 2 k\Omega \times \eta_{ADP} \times t_{step}}_{\text{Power from SMFC}}}_{\text{J added to storage cap}} - \underbrace{0.01 \times 10^{-6} \times E_{cap,t_n} \times t_{step}}_{\text{J leaked during timestep}} \quad (1)$$

E_{cap,t_n} is the energy in the capacitor from the previous time step. For each of the three system types, we define a threshold energy E_{thresh} at which the system will power the load and the capacitor will discharge to perform a discrete operation. Opportunistic operation on discrete energy quanta is a common paradigm for a diverse array of energy harvesting systems [18, 30]. Upon completion, the capacitor will start accumulating energy until it builds up enough energy to turn on the system again (e.g., when $E_{cap} > E_{thresh}$ in Figure 14). Some key factors we identified that influence this E_{thresh} value are the minimum operating voltage of the device (V_{min}), the peak

²Specifically, the Figure 8 curve with $I_{in} = 100 \mu A$ and $V_{sys} = 3 V$ (which is both the most efficient configuration and the minimum voltage that satisfies all of our application scenarios) from <https://www.analog.com/media/en/technical-documentation/data-sheets/ADP5091-5092.pdf>.

active current draw (I_{peak}), the total energy used per event (E_{event}), the amount of time required to perform the operation (t_{active}), and (when operating intermittently) the startup time ($t_{startup}$). These system parameters for our representative examples are listed in [Table 4](#):

Table 4. Power requirements for a representative suite of energy harvesting applications. Note the varying peak voltage, peak current, and duration across tiers of energy-harvesting applications. The E_{event} sum includes active and startup costs, assuming fully intermittent operation. As it draws such little power, the computational material-based system can run continuously, rendering E_{event} moot, and suggesting that SMFCs and computational materials may be very well matched.

Application	V_{min} [V]	I_{peak} [mA]	E_{event} [mJ]	t_{active} [ms]	$t_{startup}$ [ms]
<i>Advanced</i> : Sense & LoRa [44]	2.4	128	768	2500	5
<i>Minimal</i> : BLE Advertisement [17]	0.9	12.4	0.0039	0.888	(not given)
<i>Analog</i> : Analog Sense & Backscatter [11] [†]	0.11	0.0035	N/A	N/A	N/A

[†] For $f = 500$ kHz

5.1.2 Results. We used our simulation framework to explore the performance of each system, running all three devices in our trace-driven simulator across 161 days of continuous data. [Figure 15](#) illustrates the daily number of discrete events our intermittent devices could complete given the energy input from our v3 SMFCs. The number of operations each system executed is linked to the health of the SMFC, and sharp drops in the number of operations can be associated with the drying periods described in [Section 3.5](#). Regardless, the power output from a single v3 cell is enough to activate a wide range of devices for a significant portion of time while the surrounding moisture level is sufficiently high.

Due to the low power requirement of MARS, it is able to sustain continuous operation during the majority of the 161-day simulation. [Figure 16](#) examines how often MARS would run assuming it was directly powered by the SMFC with no harvesting or storage. We calculate this by finding the total energy produced over the 161-day experiment and using that to estimate the average power generation. For v3 and v0, the average power generation is 26.5 μ W and 14.7 μ W respectively, which is well above the 0.385 μ W required to keep MARS continuously powered assuming an ideally-sized and adaptive capacitor (i.e., no energy is lost and events run as soon as enough energy is available).

The energy use of MARS is so low that once it turns on, it could stay on forever. This means that sufficient energy could theoretically be accumulated to weather all of the harvesting droughts through the use of storage capacitors. In fact, the v3 cell generated on average **68** times more power than needed for the MARS tag to operate, and increased its theoretical runtime by **120%** compared to the baseline v0 cell in [Figure 16](#). This raises the question of what more sophisticated function or circuitry might be supported on an analog backscatter computational material, or if multiple MARS tags with redundant or complementary sensor load-outs could be powered by a single MFC tag and fanned around a small area to increase spatial resolution and signal fidelity. This incredibly low-power operating point is highly useful for measuring volatile and dynamic data streams that benefit from continuous sensing, which would not be possible with the other computing paradigms. However, its simple nature means that it is restricted to wirelessly delivering a constant stream of data. On the other hand, microcontroller-based systems are capable of much more complex and flexible, context-sensitive operations.

When compared to the systems powered by the baseline v0 cell, systems powered by v3 cells are able to achieve a roughly **40%** increase in total operation count across the board (43.2% for Advanced and 41.7% for Minimal), further contextualizing our new SMFC design's improved robustness to VWC (see [Figure 17](#)). Although the v3 cell's increased operating range is only 4% from a VWC standpoint, this translates to a considerable increase in the amount of computing the design enables. The difference in the number of operations achieved is especially significant after the first drying period since v3 cells feature a better recovery rate and are more robust to changes

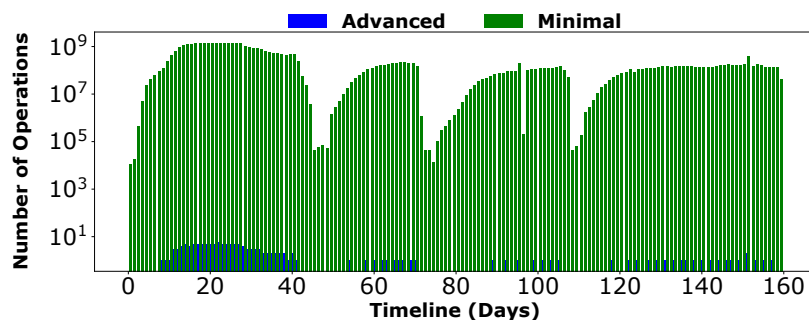


Fig. 15. Daily number of operations achieved on the Advanced and Minimal system given power from a v3 cell.

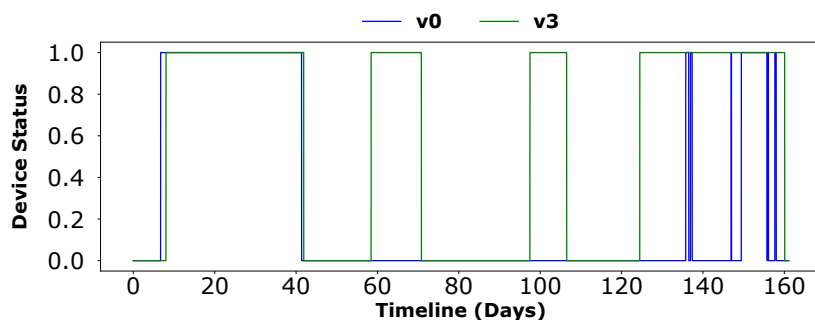


Fig. 16. On/off behavior of the computational material if wired directly to the SMFC (1 represents ON while 0 represents OFF). The energy demand of the computational material is so low that it does not require boosting circuitry or other traditional energy harvesting frontend components. However, if a storage capacitor was introduced, the SMFC produces sufficient energy to power MARS continuously throughout the whole 161-day experimental period. v3 remained in the ON state 120% longer than v0 in this simulation.

in VWC. Further, there is a large discrepancy between the number of achievable operations between the Minimal and Advanced configurations. Since the number of operations is so low for the Advanced setup due to its high energy cost, the difference between the v0 and v3 cell performances became less obvious.

5.1.3 Discussion. From the results we obtained in this simulation, we conclude that the new v3 cell design is more suitable for computing due to its ability to achieve an over **40%** boost in the number of operations each digital system (i.e., Advanced and Minimal) can execute while giving the Analog system a **120%** increase in runtime. We also determined that analog backscatter-based systems (i.e., MARS) offer the most reliable theoretical performance among the systems benchmarked in terms of computational availability because a SMFC can often exceed the computational device's energy demand. While MARS requires orders of magnitude less energy than even the lowest-power microcontroller, it is restricted to just sending a steady data stream (via backscatter with a monostatic sensing range of 12 m on a 20 kHz bandwidth [11]) and cannot handle advanced computations the way a digital device can. However, given the low and intermittent nature of SMFC's power output, the additional capabilities provided by more energy-intensive systems could be over-provisioned for distributed sensing purposes, and have low utility in the field due to missed sensor readings. In this next section, we evaluate the power production of a v3 SMFC under non-ideal field conditions to identify which of the three system types (Advanced, Minimal, Analog) it can realistically support.

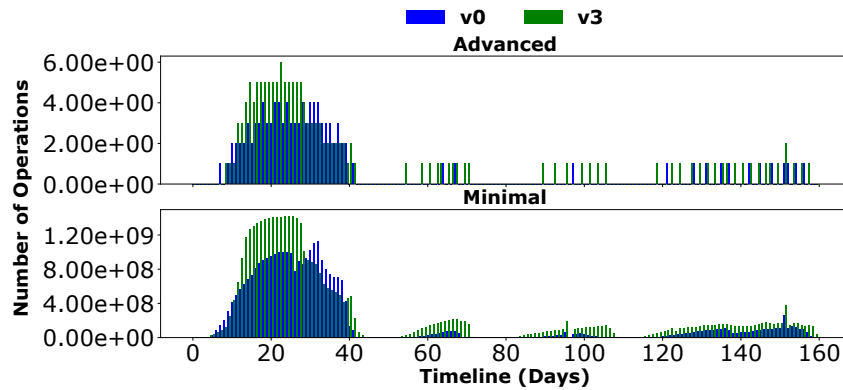


Fig. 17. The daily number of operations from the Minimal and Advanced configurations powered by either a v0 or v3 cell.

5.2 Outdoor Evaluation

Although the v3 cells from Section 3.5 have been shown to produce upwards of $50 \mu\text{W}$ after being dried out, they were evaluated under controlled settings where the soil was kept flooded for weeks at a time to revive them back to their maximum output after each drying cycle, which is unrealistic for most applications. To examine our improved v3 SMFC under field conditions, we deploy a modified v3 cell (v3.1) outside in an irrigated yard to gauge its performance and understand the impacts of real-world stimuli on SMFC power output.

5.2.1 Method. Prior to setting up the experiment, we modified the v3 cell design from Section 3.5.2 to address some of the mechanical issues it faced in lab deployments, namely leakage into the air chamber and the scaffold breaking during installation/extraction (see Figure 18). The stainless steel flange and fasteners were replaced with a monolithic 3D-printed snap-fit flange, and the scaffold was also bolstered with additional fillets and supports to increase its strength and decrease the number of openings for water to infiltrate through. A cap was added to the top of the scaffold to prevent rainwater and debris from entering the air chamber while still allowing for airflow. The scaffold, flange, cap, and anode G-clips were all 3D printed from plant-based PLA plastic to reduce the number of store-bought parts. All of the membrane and electrode materials, geometries, and configurations were kept the same as the v3 design, ensuring minimal impact on cell behavior. We will refer to this mechanically more robust version of the v3 cell as v3.1 in the rest of this work.

The deployment site for this experiment is a residential yard at a location with hot-summer Mediterranean climate (USDA Zone 10a). The surrounding environment is highly arid, with all of the non-desert plants being regularly irrigated to keep them alive. This location was chosen to observe the effects of irrigation (or the lack thereof) on SMFCs in naturally dry environments, which has been a highly-motivating application for smart agricultural sensors. To jump-start the experiment, we first incubated the v3.1 cell under inundated conditions in the lab with soil collected from the deployment site until the cell reached a steady-state voltage of about 600 mV, which was approximately the maximum of what the v3 SMFCs achieved in Section 3.5.3. The cell was loaded with a $2 \text{ k}\Omega$ resistor during incubation and throughout the entire deployment.

After incubation, the v3.1 cell was installed at the deployment site under the shade of a potted pygmy date palm (*Phoenix roebelenii*). It was carefully placed into a hole with its incubation soil intact to reduce disruptions to the anode biofilm. Otherwise, the cell was kept in an open environment with no external barrier underground (see Figure 19). The cell was irrigated through both drip irrigation and manual watering depending on the need of the tree. The soil moisture data was collected with a METER TEROS 12 sensor, while the cell's voltage and current were measured with an INA219 power monitor (Adafruit INA219).

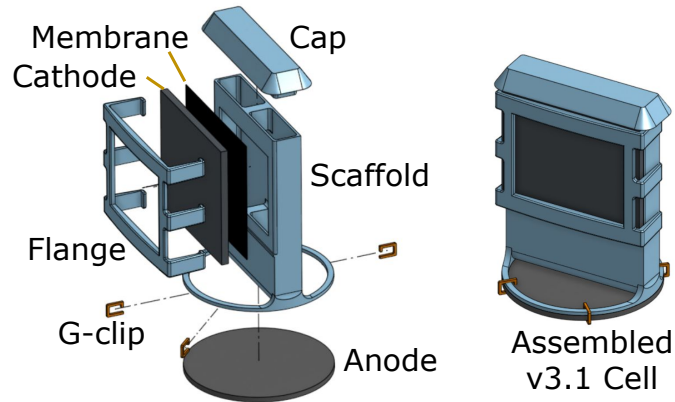


Fig. 18. Exploded and assembled view of the v3.1 SMFC modified from v3 cells to make it leak-proof and improve its mechanical strength for outdoor deployment. All of the electrode geometry and configuration were kept the same to ensure minimal impact on cell behavior.



Fig. 19. Top view of the v3.1 cell buried outside in an irrigated residential yard. The v3.1 cell is covered with a 3D-printed cap that prevents debris from entering while allowing for airflow.

5.2.2 Results. The v3.1 cell's power output dropped dramatically after being transplanted outside (see Figure 20). The red dashed line was linearly interpolated to represent the data gap from the time it took to install the SMFC. Within a day of deployment, power decreased from $186 \mu\text{W}$ to just $4 \mu\text{W}$, with a nearly $55 \mu\text{W}$ drop attributed to the deployment process itself. This is likely a result of oxygen infiltration to the anode when the cell was transported, which caused the anoxic exoelectrogenic biofilm to suffer and the cell potential to drop. However, the cell does not die completely, as its power noticeably increases whenever the VWC spikes after rain or irrigation. It was observed that the cell produces essentially zero power below 39% VWC, which roughly aligns with the 40-41% cutoff observed in the lab. This slightly lower VWC cutoff may be due to the difference in water holding capacities between the outdoor and lab soils [26], which affects the amount of water available to organisms at the same VWC.

5.2.3 Discussion. The v3.1 cell's much lower energy output post-deployment indicates that it would not be sufficient to power the Advanced or even Minimal digital systems from Section 5.1. However, it may still produce sufficient power for certain digital components like real-time clocks (which can function with just $14 \text{ nA} \times 1.5 \text{ V} = 21 \text{ nW}$ [5]) without accounting for loss from boosting voltage. The v3.1 cell's power regularly

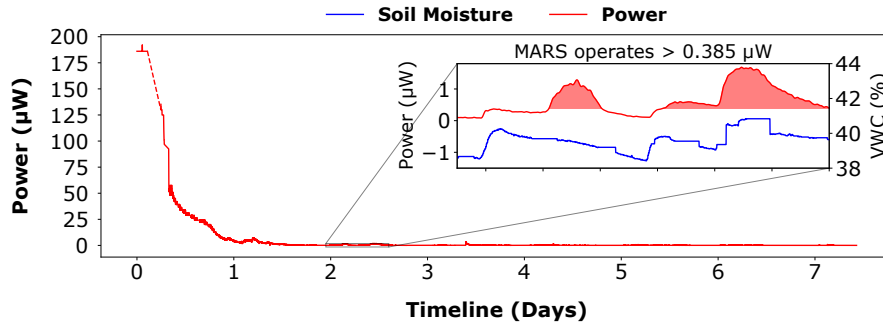


Fig. 20. The power level of the incubated v3.1 cell dropped significantly after being transplanted outside. However, it still produces enough power to theoretically turn on MARS during spikes in moisture levels caused by occasional irrigation (see shaded red regions for the energy usable by MARS [11]). This amount of power is also within the envelope of many common subsystems (i.e., a real-time clock [5]) of modern computing, showing promise.

jumps up to $>1 \mu\text{W}$ for hours at a time with a maximum of $3.5 \mu\text{W}$ during spikes in VWC caused by irrigation events, which is also potentially enough for analog backscatter sensors like MARS that require as little as $0.385 \mu\text{W}$ [11]. This indicates that the v3.1 SMFC can potentially support sensing and computing even under highly irregular moisture variations. We demonstrate connecting MARS to a SMFC for wireless sensing in the next section to examine the minimum SMFC output required to turn on MARS without additional power conditioning circuitry and showcase potential applications.

5.3 Soil-Powered Backscatter Sensor Demonstrations

This section examines the potential of soil-powered backscatter sensors by integrating the improved v3.1 SMFC design (see Section 5.2.1) with MARS tags. We explain the system that uses the energy provided by a SMFC to transmit data wirelessly, then we evaluate the runtime of MARS connected to a v3.1 cell across a range of VWC levels. Finally, we demonstrate soil moisture and touch sensing using these SMFC-powered MARS tags.

5.3.1 System. The overall system consists of a backscatter sensor and two Software Defined Radios (Great Scott Gadgets HackRF One) for either transmitting the incident wave (Tx) or receiving the backscattered signal (Rx). The backscatter sensor includes a modified Colpitts oscillator tuned to resonate at 200 kHz using a zero threshold MOSFET (ALD110800) as the amplifier (see Figure 21). A 200 kHz base oscillation frequency was chosen because it has been well-characterized to work with a sufficiently low startup voltage (110 mV). This oscillation frequency (f_{MARS}) is a function of the capacitance and inductance values in the LC tank circuit [11].

The AC output of the modified Colpitts oscillator is then fed into the gate of a depletion mode N-channel JFET transistor (MPF102), which acts as an RF switch to modulate the backscattered signal. We power this circuit with a single v3.1 SMFC, and the system can backscatter sensor readings from a 10 dB, 915 MHz incident signal to a radio receiver a meter away (see Figure 22). The SMFC was incubated under inundated conditions with the MARS tag as its load until it reached 545 mV before the start of the following experiments.

5.3.2 MARS Runtime on SMFC Power. Since a SMFC's power is also a function of its load [54], we first explore the power behavior of v3.1 SMFC while loaded with MARS alongside MARS' backscatter signal continuity. A previously incubated SMFC cell was used to power a MARS tag while the cell slowly dried, and the backscatter signal was recorded for 31 days. We plot the signal-to-noise ratio (SNR) of the backscattered signal with the corresponding power and VWC measured for the SMFC during this time in Figure 23. The backscattered data is

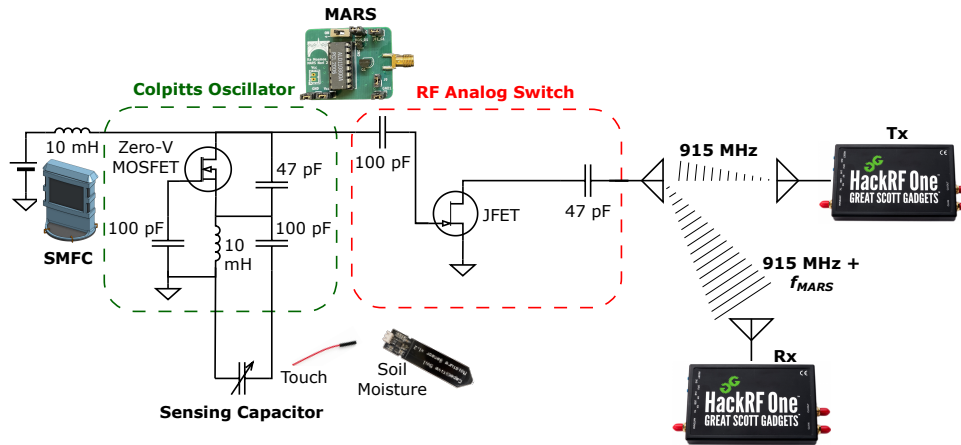


Fig. 21. SMFC+MARS system diagram. The MARS sensor includes a Colpitts oscillator that turns the low DC voltage from the v3.1 SMFC into a higher amplitude AC signal that has a frequency of f_{MARS} , which changes depending on the capacitance of the sensing capacitor. The sensing capacitor is a simple insulated wire in Section 5.3.3 and a large co-planar capacitor made from waterproof PCB in Section 5.3.4. This AC wave goes into the RF analog switch, which connects to an antenna and backscatters the f_{MARS} signal to the Rx HackRF using the 915 MHz incident signal from the Tx HackRF. This backscatter-enabled wireless capacitance sensor is entirely powered by a single SMFC.

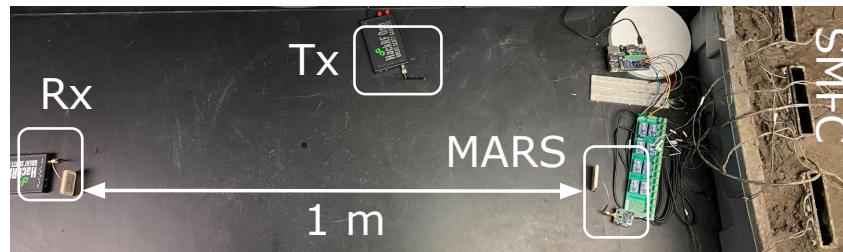


Fig. 22. Backscatter setup consisting of two patch directional antennas on MARS and Rx (Taoglas Limited ISPC.91A.09.0092E) and a monopole antenna on Tx (Great Scott Gadgets ANT500). Rx is placed 1 m away from MARS, and this distance can be extended by increasing Tx power or choosing a higher-gain antenna.

pre-processed with a moving average filter and plotted as a spectrogram. Next, the Short-Time Fourier Transform (STFT) strength of the backscattered frequency from the spectrogram is taken as the signal power and subtracted from the average noise floor to calculate the SNR. A RocketLogger [85] was used to record the voltage and current of the SMFC throughout the experiment, and VWC was captured with a METER ECH2O E-5 sensor.

As observed in Figure 23, MARS starts backscattering from day 1 with a SNR of 28.5 dB (signal strength = -71.5 dB, noise floor = -102 dB) since the SMFC's initial power ($12.8 \mu\text{W}$ at 545 mV) is well above the MARS startup requirement from literature ($0.385 \mu\text{W}$ at 110 mV) [11]. The SNR remains more or less consistent around 30 dB throughout days 1–26 regardless of power fluctuations. On day 27, a fan is installed to accelerate the drying process to observe the point at which backscattering stops. Halfway through day 29, the backscatter signal vanishes below the noise floor. At this time, the voltage of SMFC is 179.8 mV with a current of $4.34 \mu\text{A}$ ($0.781 \mu\text{W}$). The discrepancy between the power requirement from the literature and the observed output from the SMFC

when MARS turned off may be attributed to the difference between our circuit components and those used in the MARS paper. This discrepancy was also observed during the MARS tag debugging process, where it would only start operating at 180 mV and above. Regardless, $0.781 \mu\text{W}$ remains within what the v3.1 cell can produce during outdoor deployment (see Figure 20), which means a MARS tag can still potentially turn on in the field without any power conditioning circuitry. Next, we demonstrate two useful SMFC + MARS applications for sensing.

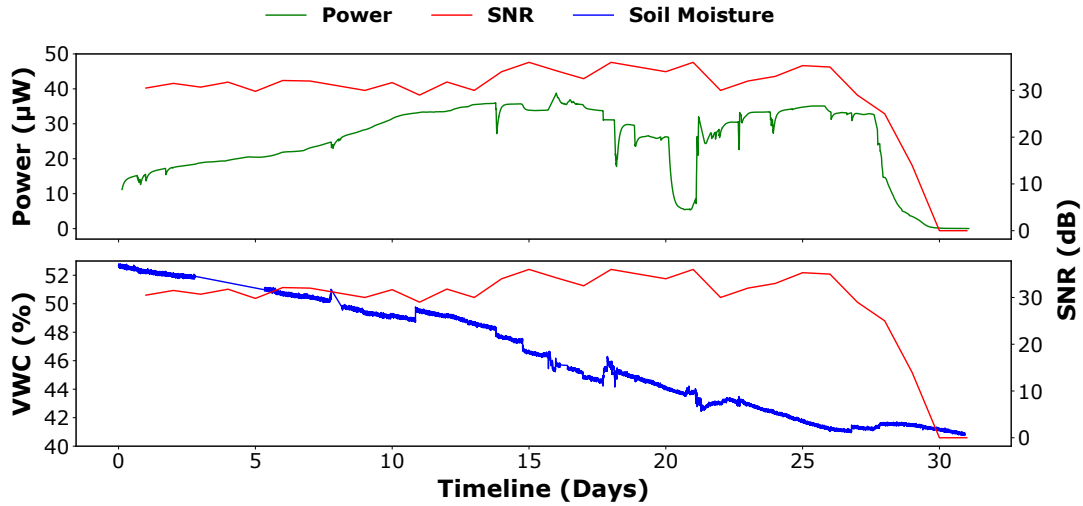


Fig. 23. Signal-to-noise ratio from MARS' 200 kHz backscatter frequency while being powered by a drying v3.1 SMFC for 30 days. The SMFC initially produced $13.8 \mu\text{W}$ at 545 mV and 52.7% VWC, and the SNR remained relatively stable throughout the entire drying process until the signal disappeared on day 30 when the SMFC power dropped to $0.781 \mu\text{W}$ at 179.8 mV and 41.5% VWC. Although this minimum operating output was higher than predicted from Section 5.2, it still falls within the typical 1–1.5 μW that the v3.1 cell produced outside during irrigation, making operating MARS tags possible even in the field.

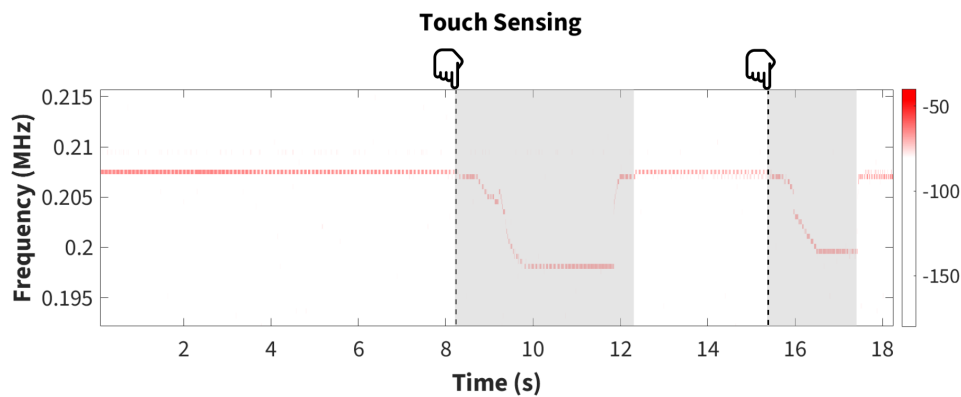


Fig. 24. Touch sensing with MARS powered by a v3.1 SMFC. The shaded areas indicate when the sensing wire (a 24 AWG Dupont jumper wire) was touched by a human hand, and the increased capacitance from the hand caused the backscatter frequency to decrease.

5.3.3 Touch Sensing. One basic capability of the soil-powered backscatter sensor is touch sensing. As f_{MARS} is dependent on the capacitance of the Colpitts oscillator's LC tank, attaching a simple insulated wire to the device effectively introduces a variable capacitor that acts as a sensor. When the wire is in contact with another object, the capacitance of the wire increases, resulting in a lower f_{MARS} detected by Rx [11]. In Figure 24, a user grabbed the sensing wire with their hand twice, which correlates with the two dips in backscatter frequency.

Since the fringing field of a cylindrical capacitor (the wire) is very small, only items very close to or directly touching the wire will change its capacitance, making it robust to noise. This configuration provides a binary measurement for whether something is in contact with the wireless sensor, which can be useful for applications like wildlife monitoring. By placing such a device flush with the forest floor, one may be able to create a low-profile soil-powered sensor that perpetually operates to detect whether it has been stepped on by animals. Although solar-powered sensors will perform poorly under dense tree canopies and potential overhead debris, SMFCs require no light and can continue to operate as long as the cathode is not completely buried.

5.3.4 Soil Moisture Sensing. Another practical application of this variable capacitor is soil moisture sensing. To detect changes in the VWC, we adopt a coplanar capacitor that extends into the bulk soil as the sensing capacitor. The co-planar capacitor is built by modifying a commercial capacitive soil moisture sensor (DFROBOT SEN0193) so that one of its insulated copper plates connects directly to the LC tank and the other connects to the ground of the MARS tag. When the surrounding VWC changes, the absolute dielectric permittivity of the soil also changes, which affects the capacitance value of the sensing capacitor. This change in C shifts the frequency of the Colpitts oscillator, essentially encoding the soil moisture content into a frequency value.

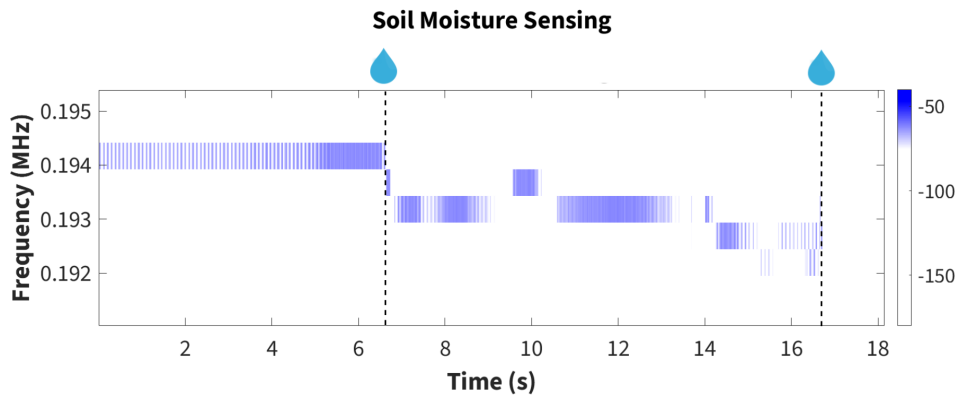


Fig. 25. Soil moisture sensing with MARS powered by a v3.1 SMFC. The soil VWC was increased during each watering event. The backscatter frequency changed steadily from 0.194 MHz to 0.192 MHz in the first watering event due to the increasing capacitance of the sensor, and the capacitance exceeded the upper threshold required for the Colpitts oscillator to oscillate during the second watering event, which caused the backscatter signal to disappear.

In Figure 25, the moisture sensor connected to MARS was buried in dry sieved soil. Approximately 2 mL of deionized water was poured on the soil near the sensor during each of the two watering events denoted by the black dashed lines. During the first watering event, the backscatter frequency dropped steadily by 2 kHz, and in the second watering event, the backscatter signal disappeared entirely. This is because the additional capacitance imposed by the sensor to the LC tank exceeded the limit for the Colpitts oscillator to remain stable, which brought f_{MARS} to zero. By tuning the geometry and capacitance of the moisture sensor, one can adjust the resolution of the VWC reading and even set a threshold VWC at which the backscatter signal cuts off, alerting the Rx device of overwatering or extreme rain events. This potentially makes the soil-powered MARS sensor a powerful choice for

VWC sensing and flood detection in wetland and green infrastructure monitoring applications where batteries and solar panels face issues from corrosion and chemicals leaching out.

5.3.5 Discussion. The proof-of-concept systems from Sections 5.3.3 and 5.3.4 demonstrate the viability of using SMFCs to power wireless sensors, especially simple analog backscatter devices like MARS. These analog sensors can run on a single SMFC without any additional power conditioning and bring critical sensing capabilities like touch and water detection into wildlife, agricultural, and green infrastructure monitoring applications where SMFCs may thrive. With the advent of organic transistors and plant-based circuit components [22, 89, 93], simple two-transistor designs like MARS can potentially be made entirely compostable, which combined with a biomass-based SMFC enables the creation of fully-biodegradable, self-powered wireless environmental sensors. These devices can then be deployed at scale to provide high-quality data without worrying about the impacts of littering the environment with e-waste. Although there are still practical issues that need to be resolved, such as improving backscatter communication range and SMFC power continuity, this soil-powered backscatter system establishes a foundation that holds promise to bring a new level of sustainability to ubiquitous computing.

6 DISCUSSION & FUTURE WORK

The envisioned future work is geared towards encouraging and enabling community research involvement that takes our contributions and builds on top of them to make soil-powered ubiquitous computing a reality. This vision is far off, requiring many more insights and explorations. We discuss some challenges, goals, and mechanisms that our framework and contributions can bring to future researchers below.

Although our effort focused on improving SMFC's overall robustness to soil moisture changes to increase their power output, many of our findings from Sections 3 and 4 can be generalized to design cells for other useful traits as well (resilience to temperature changes, soil types, etc.). Researchers who wish to install SMFCs in colder climates may need to modify their design to boost anode activity during the winter months, and leveraging our debugging framework from Section 4.1 and experimental guide from Appendix A.2 would allow them to rapidly identify issues and get cells ready for deployment. SMFC design is a complex iterative process due to the conundrum of factors that are known to affect their behavior, but not fully characterized by existing literature (see Section 2.1.4). Even the v3.1 prototype produced at the end of our iteration cycle falls short of what is needed to bring SMFCs into many applications, since its high 41% VWC requirement restricts cell activity to only when the soil is nearly saturated to field capacity [26]. The outdoor deployment in Section 5.2 likewise confirmed v3.1 SMFCs' limited power production in the field, suggesting that further design changes are necessary.

This ongoing challenge to stabilize SMFC power output for computing applications precisely highlights the importance of open-sourced work that focuses on community enablement. The data produced from this study can be used in future experiments to model SMFC power from complex environmental inputs with machine learning. This may not only allow researchers to predict cell designs, but also be used in-situ for reinforcement learning based tuning of computing tasks given the predicted SMFC performance. Early stage work on MFC modeling with machine learning is already underway [7], making MFC data containing characterized relationships with environmental parameters especially important. SMFC research is highly interdisciplinary, so increasing the transparency and reproducibility of experiments will allow the field to engage experts from more diverse backgrounds to realize a soil-powered vision.

Continuing this concept of community enablement and reproducibility, additional tools can be developed in future work to facilitate more replicable experiments. Since SMFCs react to changes on such a local scale, it is very difficult to ensure accurate VWC measurements and truly homogenous soils using existing resources, resulting in unavoidable discrepancies between and even within experiments. Current commercial soil moisture sensors typically give bulk readings for a large volume. This, in combination with SMFC's small size, makes it impossible to accurately determine the moisture level in specific components of the SMFC, which can be critical

in understanding the soil water dynamics within the cell. Having a precise gradient of water content within a SMFC will give better insights into how one can keep them operating through droughts. Lastly, because soil composition varies between every location, researchers currently cannot reasonably compare their SMFC design's absolute power production with a SMFC deployed elsewhere even if the temperature and moisture are held exactly the same. Creating a standard "synthetic soil" akin to the synthetic wastewater that exist in aqueous MFC work [71] would advance the level of reproducibility in SMFC experiments, as true direct design comparisons can only be done when all else is equal, including the soil.

7 CONCLUSIONS

This work sought to jump-start the field of soil-powered computing by establishing the gaps in current SMFC development, iterating through 4 cell designs to improve their robustness, extracting general guidelines and key lessons learned from our experiments, and evaluating the improved SMFC design using an outdoor deployment, simulation, and integration with real backscatter sensors. We describe a 2-year-long design iteration process in which four different SMFC cell concepts were tested to improve upon the flat conventional SMFC design to increase their utility for powering computing and sensing tasks. Using our fundamental knowledge of MFCs and our direct comparison method, we addressed the shortcomings of the v0 design one by one to develop a functional v3 prototype that is more robust to changes in soil moisture. We collected a combined nine months' worth of SMFC performance data, which we used to simulate the theoretical runtime of different computing form factors (Advanced, Minimal, and Analog systems) to compare their relative performances. The simulation showed that just 4% improvement in the operational VWC range from the v3 cell increased its overall potential computing operation count by 40% for digital systems and over 120% for the runtime of analog systems like MARS. We further assessed the real-world viability of SMFCs by deploying a mechanically modified v3 cell (v3.1) in an irrigated residential yard and connecting it to ultra-low power backscatter sensors in the lab to demonstrate soil-powered wireless touch and moisture sensing.

While there are still many obstacles to powering practical computing systems with SMFCs at this stage in development, SMFCs show significant promise as a sustainable, potentially biodegradable ambient harvesting source that generates enough energy to power analog wireless sensors long-term. The v3.1 cell power hovered around 1-1.5 μW in the field during irrigation, which is greater than the minimum 0.781 μW required to turn on MARS in our lab experiment. We contribute all of our finalized designs, building tutorials, and simulation tools online³ so we may open the door for further research to allow SMFC-powered sensors to fill the computing community's need for sustainable, self-powered IoT devices.

ACKNOWLEDGMENTS

This material is based upon work supported by the National Science Foundation under Grant No. CNS-2038853. Any opinions, findings, conclusions, or recommendations expressed in this material are those of the authors and do not necessarily reflect the views of the National Science Foundation or other supporters. This work is also supported by Agricultural and Food Research Initiative grant no. 2023-67021-40628 from the USDA National Institute of Food and Agriculture. We would further like to acknowledge support by the Alfred P. Sloan Foundation, VMware Research, and 3M. We thank our peers from the Wells Lab and Rapid Prototyping Lab at Northwestern for their support in manufacturing SMFCs. We also want to thank Eric Greenlee, Yuhui Zhao, and Yaman Sangar from the Ka Moamoia Lab for their assistance in building MARS tags. The authors gratefully acknowledge valuable manuscript feedback from Raj Amirtharajah and Tinyu Cheng.

³We release all mechanical designs and simulation tools at https://github.com/ka-moamoia/Practical_SMFC_Design_Guide.

REFERENCES

- [1] 2018. Silica Statistics and Information. <https://www.usgs.gov/centers/national-minerals-information-center/silica-statistics-and-information#:~:text=In%20almost%20all%20cases%2C%20silica,usually%20has%20limited%20environmental%20impact>.
- [2] 2020. Reference Electrodes. [https://chem.libretexts.org/Bookshelves/Analytical_Chemistry/Supplemental_Modules_\(Analytical_Chemistry\)/Analytical_Sciences_Digital_Library/Courseware/Analytical_Electrochemistry%3A_Potentiometry/03_Potentiometric_Theory/04_Reference_Electrodes#:~:text=Silver%2FSilver%20Chloride%20\(Ag%2FAgCl\),-The%20silver%2Fsilver&text=with%20a%20value%20for%20E,which%20is%20not%20exactly%20unity](https://chem.libretexts.org/Bookshelves/Analytical_Chemistry/Supplemental_Modules_(Analytical_Chemistry)/Analytical_Sciences_Digital_Library/Courseware/Analytical_Electrochemistry%3A_Potentiometry/03_Potentiometric_Theory/04_Reference_Electrodes#:~:text=Silver%2FSilver%20Chloride%20(Ag%2FAgCl),-The%20silver%2Fsilver&text=with%20a%20value%20for%20E,which%20is%20not%20exactly%20unity).
- [3] 2022. Cleaning Up Electronic Waste (E-Waste). <https://www.epa.gov/international-cooperation/cleaning-electronic-waste-e-waste>
- [4] 2022. End-of-Life Solar Panels: Regulations and Management. <https://www.epa.gov/hw/end-life-solar-panels-regulations-and-management#Are%20Solar%20Panels%20Hazardous%20Waste?>
- [5] 2023. Artasie Real-Time Clock - AM1805. <https://ambiq.com/artasie-am1805/>
- [6] 2023. MudWatt: Grow a Living Fuel Cell. <https://www.magicalmicrobes.com/products/mudwatt-clean-energy-from-mud>
- [7] Yaser Abdollahfard, Mehdi Sedighi, and Mostafa Ghasemi. 2023. A New Approach for Improving Microbial Fuel Cell Performance Using Artificial Intelligence. *Sustainability* 15, 2 (2023), 1312.
- [8] SC Abrahams and K Nassau. 1991. Piezoelectric Materials. *Concise Encyclopedia of Advanced Ceramic Materials* (1991), 351–354.
- [9] Mikhail Afanasov, Naveed Bhatti, Dennis Campagna, Giacomo Caslini, Fabio Massimo Centonze, Koustabh Dolui, Andrea Maioli, Erica Barone, Muhammad Hamad Alizai, Junaid Haroon Siddiqui, and Luca Mottola. 2020. Battery-less Zero-maintenance Embedded Sensing at the Mithraeum of Circus Maximus. In *Proceedings of the 18th Conference on Embedded Networked Sensor Systems (SenSys '20)*. Association for Computing Machinery, New York, NY, USA, 1–14.
- [10] Wilgince Apollon, Sathish-Kumar Kamaraj, Héctor Silos-Espino, Catarino Perales-Segovia, Luis L Valera-Montero, Víctor A Maldonado-Ruelas, Marco A Vázquez-Gutiérrez, Raúl A Ortiz-Medina, Silvia Flores-Benítez, and Juan F Gómez-Leyva. 2020. Impact of *Opuntia* species plant bio-battery in a semi-arid environment: Demonstration of their applications. *Applied Energy* 279 (2020), 115788.
- [11] Nivedita Arora, Ali Mirzazadeh, Injoo Moon, Charles Ramey, Yuhui Zhao, Daniela C Rodriguez, Gregory D Abowd, and Thad Starner. 2021. MARS: Nano-Power Battery-free Wireless Interfaces for Touch, Swipe and Speech Input. In *The 34th Annual ACM Symposium on User Interface Software and Technology*. 1305–1325.
- [12] Daniel Ayala-Ruiz, Alejandro Castillo Atoche, Erica Ruiz-Ibarra, Edith Osorio de la Rosa, and Javier Vázquez Castillo. 2019. A self-powered PMFC-based wireless sensor node for smart city applications. *Wireless Communications and Mobile Computing* 2019 (2019).
- [13] Abu Bakar, Rishabh Goel, Jasper de Winkel, Jason Huang, Saad Ahmed, Bashima Islam, Przemyslaw Pawelczak, Kasim Sinan Yildirim, and Josiah Hester. 2022. Protean: An Energy-Efficient and Heterogeneous Platform for Adaptive and Hardware-Accelerated Battery-Free Computing. In *Proceedings of the 20th ACM Conference on Embedded Networked Sensor Systems (SenSys '22)*. 207–221.
- [14] Abu Bakar, Alexander G Ross, Kasim Sinan Yildirim, and Josiah Hester. 2021. Rehash: A flexible, developer focused, heuristic adaptation platform for intermittently powered computing. *Proceedings of the ACM on Interactive, Mobile, Wearable and Ubiquitous Technologies* 5, 3 (2021), 1–42.
- [15] Paul Basore and David Feldman. 2022. *Solar Photovoltaics-Supply Chain Deep Dive Assessment*. Technical Report. USDOE Office of Policy (PO).
- [16] David Benedetti, Chiara Petrioli, and Dora Spenza. 2013. GreenCastalia: An energy-harvesting-enabled framework for the Castalia simulator. In *Proceedings of the 1st International Workshop on Energy Neutral Sensing Systems*. 1–6.
- [17] Bradford Campbell, Joshua Adkins, and Prabal Dutta. 2016. Cinamin: A Perpetual and Nearly Invisible BLE Beacon. In *International Conference on Embedded Wireless Systems and Networks (EWSN)*.
- [18] Bradford Campbell and Prabal Dutta. 2014. An energy-harvesting sensor architecture and toolkit for building monitoring and event detection. In *Proceedings of the 1st ACM Conference on Embedded Systems for Energy-Efficient Buildings (BuildSys'14)*. ACM, New York, NY, USA, 100–109. <https://doi.org/10.1145/2674061.2674083>
- [19] Armande Capitaine, Gael Pillonnet, Thibaut Chailloux, Adrien Morel, and Bruno Allard. 2017. Impact of switching of the electrical harvesting interface on microbial fuel cell losses. In *IEEE SENSORS*. <https://doi.org/10.1109/ICSENS.2017.8234189>
- [20] Martin H Chantigny. 2003. Dissolved and water-extractable organic matter in soils: a review on the influence of land use and management practices. *Geoderma* 113, 3–4 (2003), 357–380.
- [21] B Chen, W Cai, and A Garg. 2023. Relationship between bioelectricity and soil–water characteristics of biochar-aided plant microbial fuel cell. *Acta Geotechnica* (2023), 1–14.
- [22] Chaoji Chen, Ying Zhang, Yiju Li, Jiaqi Dai, Jianwei Song, Yonggang Yao, Yunhui Gong, Iain Kierzewski, Jia Xie, and Liangbing Hu. 2017. All-wood, low tortuosity, aqueous, biodegradable supercapacitors with ultra-high capacitance. *Energy & Environmental Science* 10, 2 (2017), 538–545.
- [23] Alexei Colin, Emily Ruppel, and Brandon Lucia. 2018. A reconfigurable energy storage architecture for energy-harvesting devices. In *Proceedings of the Twenty-Third International Conference on Architectural Support for Programming Languages and Operating Systems*.

- 767–781.
- [24] Pierangela Cristiani, Iwona Gajda, John Greenman, Francesca Pizza, Paolo Bonelli, and Ioannis Ieropoulos. 2019. Long term feasibility study of in-field floating microbial fuel cells for monitoring anoxic wastewater and energy harvesting. *Frontiers in Energy Research* 7 (2019), 119.
- [25] Katarzyna Dabrowska-Zielinska, Jan Musial, Alicja Malinska, Maria Budzynska, Radoslaw Gurdak, Wojciech Kiryla, Maciej Bartold, and Patryk Grzybowski. 2018. Soil moisture in the Biebrza Wetlands retrieved from Sentinel-1 imagery. *Remote Sensing* 10, 12 (2018), 1979.
- [26] Sumon Datta, Saleh Taghvaeian, and Jacob Stivers. 2018. Understanding soil water content and thresholds for irrigation management - Oklahoma State University. <https://extension.okstate.edu/fact-sheets/understanding-soil-water-content-and-thresholds-for-irrigation-management.html>
- [27] Frank A de Carvalho, Juliana NP Nobre, Rosana P Cambraia, Alexandre C Silva, José D Fabris, Arlete B dos Reis, and Bernat V Prat. 2021. Quartz mining waste for concrete production: environment and public health. *Sustainability* 14, 1 (2021), 389.
- [28] Jasper De Winkel, Vito Kortbeek, Josiah Hester, and Przemyslaw Pawelczak. 2020. Battery-free game boy. *Proceedings of the ACM on Interactive, Mobile, Wearable and Ubiquitous Technologies* 4, 3 (2020), 1–34.
- [29] Eimear Deady, Charlie Moon, Kathryn Moore, Kathryn M Goodenough, and Robin K Shail. 2022. Bismuth: Economic geology and value chains. *Ore Geology Reviews* 143 (2022), 104722.
- [30] Samuel DeBruin, Bradford Campbell, and Prabal Dutta. 2013. Monjolo: An Energy-harvesting Energy Meter Architecture. In *Proceedings of the 11th ACM Conference on Embedded Networked Sensor Systems (SenSys'13)*. ACM, New York, NY, USA, Article 18, 14 pages. <https://doi.org/10.1145/2517351.2517363>
- [31] Conrad Donovan, Alim Dewan, Deukhyoun Heo, and Haluk Beyenal. 2008. Batteryless, wireless sensor powered by a sediment microbial fuel cell. *Environmental science & technology* 42, 22 (2008), 8591–8596.
- [32] Sara J Dunaj, Joseph J Vallino, Mark E Hines, Marcus Gay, Christine Kobyljanec, and Juliette N Rooney-Varga. 2012. Relationships between soil organic matter, nutrients, bacterial community structure, and the performance of microbial fuel cells. *Environmental Science & Technology* 46, 3 (2012), 1914–1922.
- [33] Jakub Dziegielowski, Benjamin Metcalfe, Paola Villegas-Guzman, Carlos A Martínez-Huitle, Adryane Gorayeb, Jannis Wenk, and Mirella Di Lorenzo. 2020. Development of a functional stack of soil microbial fuel cells to power a water treatment reactor: From the lab to field trials in North East Brazil. *Applied Energy* 278 (2020), 115680.
- [34] Shahjadi Hisan Farjana, Nazmul Huda, and MA Parvez Mahmud. 2019. Life cycle assessment of cobalt extraction process. *Journal of Sustainable Mining* 18, 3 (2019), 150–161.
- [35] Matthew Furlong, Josiah Hester, Kevin Storer, and Jacob Sorber. 2016. Realistic simulation for tiny batteryless sensors. In *Proceedings of the 4th International Workshop on Energy Harvesting and Energy-Neutral Sensing Systems*. 23–26.
- [36] Kai Geissdoerfer and Marco Zimmerling. 2022. Learning to communicate effectively between battery-free devices. In *19th USENIX Symposium on Networked Systems Design and Implementation (NSDI 22)*. 419–435.
- [37] Cihan Berk Güngör, Patrick P. Mercier, and Hakan Töreyn. 2021. A 3.75 nW Analog Electrocardiogram Processor Facilitating Stochastic Resonance for Real-Time R-wave Detection. In *2021 IEEE Biomedical Circuits and Systems Conference (BioCAS)*. 1–6. <https://doi.org/10.1109/BioCAS49922.2021.9645028>
- [38] Theo Henckens. 2021. Chapter 7 - Thirteen scarce resources analyzed. In *Governance of the World's Mineral Resources*, Theo Henckens (Ed.). Elsevier, 147–380. <https://doi.org/10.1016/B978-0-12-823886-8.00007-5>
- [39] Carolyn Hoskinson. 2023. Lithium Battery Recycling Regulatory Status and Frequently Asked Questions.
- [40] Yongsheng Huang, Daochun Xu, Jiangming Kan, and Wenbin Li. 2019. Study on field experiments of forest soil thermoelectric power generation devices. *Plos One* 14, 8 (2019), e0221019.
- [41] Sophie Theresia Huber and Karl W Steininger. 2022. Critical sustainability issues in the production of wind and solar electricity generation as well as storage facilities and possible solutions. *Journal of Cleaner Production* 339 (2022), 130720.
- [42] Rakesh Krishnamoorthy Iyer and Srikanth Pilla. 2021. Environmental profile of thermoelectrics for applications with continuous waste heat generation via life cycle assessment. *Science of The Total Environment* 752 (2021), 141674.
- [43] Dhananjay Jagtap and Pat Pannuto. 2020. Reliable Energy Sources as a Foundation for Reliable Intermittent Systems. In *Proceedings of the Eighth ACM International Workshop on Energy Harvesting and Energy-Neutral Sensing Systems (ENSys'20)*. ACM, New York, NY, USA. <https://doi.org/10.1145/3417308.3430276>
- [44] Dhananjay Jagtap and Pat Pannuto. 2021. Repurposing Cathodic Protection Systems as Reliable, in-situ, Ambient Batteries for Sensor Networks. In *Proceedings of the 20th ACM/IEEE International Conference on Information Processing in Sensor Networks (IPSN'21)*. ACM, New York, NY, USA.
- [45] Yun-Bin Jiang, Wen-Hui Zhong, Cheng Han, and Huan Deng. 2016. Characterization of electricity generated by soil in microbial fuel cells and the isolation of soil source exoelectrogenic bacteria. *Frontiers in microbiology* 7 (2016), 1776.
- [46] Shan Jin, Deying Mu, Ziang Lu, Ruhong Li, Zhu Liu, Yue Wang, Shuang Tian, and Changsong Dai. 2022. A comprehensive review on the recycling of spent lithium-ion batteries: Urgent status and technology advances. *Journal of Cleaner Production* 340 (2022), 130535.

- <https://doi.org/10.1016/j.jclepro.2022.130535>
- [47] Colleen Josephson, Neal Jackson, and Pat Pannuto. 2020. Farming Electrons: Galvanic Versus Microbial Energy in Soil Batteries. *IEEE Sensors Letters* 4, 12 (2020), 1–4. <https://doi.org/10.1109/LESENS.2020.3043666>
- [48] Colleen Josephson, Manikanta Kotaru, Keith Winstein, Sachin Katti, and Ranveer Chandra. 2021. Low-cost in-ground soil moisture sensing with radar backscatter tags. In *ACM SIGCAS conference on computing and sustainable societies*. 299–311.
- [49] Colleen Josephson, Weitao Shuai, Gabriel Marcano, Pat Pannuto, Josiah Hester, and George Wells. 2022. The Future of Clean Computing May Be Dirty. *GetMobile: Mobile Computing and Communications* 26, 3 (2022), 9–15.
- [50] Zerina Kapetanovic, Miguel Morales, and Joshua R Smith. 2022. Communication by means of modulated Johnson noise. *Proceedings of the National Academy of Sciences* 119, 49 (2022), e2201337119.
- [51] Atsushi Kouzuma, Nobuo Kaku, and Kazuya Watanabe. 2014. Microbial electricity generation in rice paddy fields: recent advances and perspectives in rhizosphere microbial fuel cells. *Applied Microbiology and Biotechnology* 98, 23 (2014), 9521–9526.
- [52] Thi Xuan Huong Le, Mikhael Bechelany, and Marc Cretin. 2017. Carbon felt based-electrodes for energy and environmental applications: A review. *Carbon* 122 (2017), 564–591.
- [53] O Lefebvre, A Uzabiaga, YJ Shen, Z Tan, YP Cheng, W Liu, and HY Ng. 2011. Conception and optimization of a membrane electrode assembly microbial fuel cell (MEA-MFC) for treatment of domestic wastewater. *Water Science and Technology* 64, 7 (2011), 1527–1532.
- [54] Fu-To Lin, Yu-Chun Kuo, Jen-Chien Hsieh, Hsi-Yuan Tsai, Yu-Te Liao, and Huang-Chen Lee. 2015. A self-powering wireless environment monitoring system using soil energy. *IEEE Sensors Journal* 15, 7 (2015), 3751–3758.
- [55] Brandon Lucia, Brad Denby, Zachary Manchester, Harsh Desai, Emily Ruppel, and Alexei Colin. 2021. Computational Nanosatellite Constellations: Opportunities and Challenges. *GetMobile: Mobile Comp. and Comm.* 25, 1 (jun 2021), 16–23. <https://doi.org/10.1145/3471440.3471446>
- [56] David Luria, Alexander Fantalkin, Ezra Zilberman, and Eyal Ben-Dor. 2020. Identifying the Brazil nut effect in archaeological site formation processes. *Mediterranean Geoscience Reviews* 2 (2020), 267–281.
- [57] Andrea Maioli and Luca Mottola. 2021. ALFRED: Virtual Memory for Intermittent Computing. In *Proceedings of the 19th ACM Conference on Embedded Networked Sensor Systems*. 261–273.
- [58] Gabriel Marcano, Colleen Josephson, and Pat Pannuto. 2022. Early Characterization of Soil Microbial Fuel Cells. In *IEEE International Symposium on Circuits and Systems (ISCAS) Special Session on Smart Agriculture (ISCAS'22)*. IEEE.
- [59] Gabriel Marcano and Pat Pannuto. 2021. Powering an E-Ink Display from Soil Bacteria. In *Proceedings of the 19th ACM Conference on Embedded Networked Sensor Systems*. 590–591.
- [60] Gabriel Marcano and Pat Pannuto. 2022. Soil Power? Can Microbial Fuel Cells Power Non-Trivial Sensors?. In *Proceedings of the 1st ACM Workshop on No Power and Low Power Internet-of-Things*. 8–13.
- [61] Catarina Lousa Marques. 2021. *Theoretical Analysis of a Potentiostat for Studying Microbial Fuel Cells*. Ph.D. Dissertation. Universidade da Beira Interior (Portugal).
- [62] Christine Minke, Ulrich Kunz, and Thomas Turek. 2017. Carbon felt and carbon fiber-A techno-economic assessment of felt electrodes for redox flow battery applications. *Journal of Power Sources* 342 (2017), 116–124.
- [63] Abdelrhman Mohamed, Eduardo Sanchez, Natalie Sanchez, Maren L Friesen, and Haluk Beyenal. 2021. Electrochemically Active Biofilms as an Indicator of Soil Health. *Journal of The Electrochemical Society* 168, 8 (2021), 087511.
- [64] Saman Naderiparizi, Mehrdad Hesar, Vamsi Talla, Shyamnath Gollakota, and Joshua R Smith. 2018. Towards battery-free HD video streaming. In *15th USENIX Symposium on Networked Systems Design and Implementation (NSDI 18)*. 233–247.
- [65] Nedat T Nassar, Haeyeon Kim, Max Frenzel, Michael S Moats, and Sarah M Hayes. 2022. Global tellurium supply potential from electrolytic copper refining. *Resources, Conservation and Recycling* 184 (2022), 106434.
- [66] Dang-Trang Nguyen, Kozo Taguchi, et al. 2021. A portable soil microbial fuel cell for sensing soil water content. *Measurement: Sensors* 18 (2021), 100231.
- [67] Hoang-Uyen-Dung Nguyen, Dang-Trang Nguyen, and Kozo Taguchi. 2021. A novel design portable plugged-type soil microbial fuel cell for bioelectricity generation. *Energies* 14, 3 (2021), 553.
- [68] Naoki Nitta, Feixiang Wu, Jung Tae Lee, and Gleb Yushin. 2015. Li-ion battery materials: present and future. *Materials today* 18, 5 (2015), 252–264.
- [69] National Oceanic and Atmospheric Administration. [n.d.]. Bismuth Telluride. *CAMEO Chemicals* ([n. d.]). <https://cameochemicals.noaa.gov/chemical/25002>
- [70] Edith Osorio-de-la Rosa, Javier Vazquez-Castillo, Alejandro Castillo-Atoche, Julio Heredia-Lozano, Andrea Castillo-Atoche, Guillermo Becerra-Nunez, and Romeli Barbosa. 2020. Arrays of plant microbial fuel cells for implementing self-sustainable wireless sensor networks. *IEEE sensors journal* 21, 2 (2020), 1965–1974.
- [71] Fatemeh Oveisi, Narges Fallah, and Bahram Nasernejad. 2021. Biodegradation of synthetic wastewater containing styrene in microbial fuel cell: Effect of adaptation of microbial community. *Fuel* 305 (2021), 121382.
- [72] Pat Pannuto, Benjamin Kempke, and Prabal Dutta. 2018. Slocalization: Sub-uW ultra wideband backscatter localization. In *2018 17th ACM/IEEE International Conference on Information Processing in Sensor Networks (IPSN)*. IEEE, 242–253.

- [73] Joseph A Paradiso and Thad Starner. 2005. Energy scavenging for mobile and wireless electronics. *IEEE Pervasive computing* 4, 1 (2005), 18–27.
- [74] Douglas Pedersen, Michael Lybbert, and Roseanne Warren. 2022. Life Cycle Analysis of LiCoO₂/Graphite Batteries with Cooling Using Combined Electrochemical-Thermal Modeling. *Resources, Conservation and Recycling* 180 (2022), 106204.
- [75] Andrea Pietrelli, Andrea Micangeli, Vincenzo Ferrara, and Alessandro Raffi. 2014. Wireless sensor network powered by a terrestrial microbial fuel cell as a sustainable land monitoring energy system. *Sustainability* 6, 10 (2014), 7263–7275.
- [76] Sudeep C Popat and César I Torres. 2016. Critical transport rates that limit the performance of microbial electrochemistry technologies. *Bioresource technology* 215 (2016), 265–273.
- [77] Michael C Potter. 1911. Electrical effects accompanying the decomposition of organic compounds. *Proceedings of the royal society of London. Series b, containing papers of a biological character* 84, 571 (1911), 260–276.
- [78] Song Qiu, Zhenyu Guo, Faiza Naz, Zhao Yang, and Changyuan Yu. 2021. An overview in the development of cathode materials for the improvement in power generation of microbial fuel cells. *Bioelectrochemistry* 141 (2021), 107834.
- [79] Benjamin Ransford, Jacob Sorber, and Kevin Fu. 2011. Mementos: System support for long-running computation on RFID-scale devices. In *Proceedings of the sixteenth international conference on Architectural support for programming languages and operating systems*. 159–170.
- [80] Bruce E Rittmann and Perry L McCarty. 2001. *Environmental biotechnology: principles and applications*. McGraw-Hill Education.
- [81] René A Rozendal, Hubertus VM Hamelers, Korneel Rabaey, Jurg Keller, and Cees JN Buisman. 2008. Towards practical implementation of bioelectrochemical wastewater treatment. *Trends in biotechnology* 26, 8 (2008), 450–459.
- [82] Joaquim Sanz, Oriol Tomasa, Abigail Jimenez-Franco, and Nor Sidki-Rius. 2022. Zirconium (Zr)[Z= 40]. In *Elements and Mineral Resources*. Springer, 255–258.
- [83] Davide Sartori and Davide Brunelli. 2016. A smart sensor for precision agriculture powered by microbial fuel cells. In *2016 IEEE Sensors Applications Symposium (SAS)*. IEEE, 1–6.
- [84] Victor Shnayder, Mark Hempstead, Bor-rong Chen, Geoff Werner Allen, and Matt Welsh. 2004. Simulating the power consumption of large-scale sensor network applications. In *Proceedings of the 2nd international conference on Embedded networked sensor systems*. 188–200.
- [85] Lukas Sigrist, Andres Gomez, Roman Lim, Stefan Lippuner, Matthias Leubin, and Lothar Thiele. 2016. Rocketlogger: Mobile power logger for prototyping iot devices: Demo abstract. In *Proceedings of the 14th ACM Conference on Embedded Network Sensor Systems CD-ROM*. 288–289.
- [86] Meshack Imologie Simeon, Abdulganiy Olayinka Raji, Gbabo Agidi, and CA Okoro-Shekwaga. 2016. Performance of a Single Chamber Soil Microbial Fuel Cell at Varied External Resistances for Electrical Power Generation. (2016).
- [87] Meshack Imologie Simeon, Alfons Weig, and Ruth Freitag. 2022. Optimization of soil microbial fuel cell for sustainable bio-electricity production: combined effects of electrode material, electrode spacing, and substrate feeding frequency on power generation and microbial community diversity. *Biotechnology for Biofuels and Bioproducts* 15, 1 (2022), 1–19.
- [88] Shikha Singh, Melanie A Mayes, Stephanie N Kivlin, and Sindhu Jagadamma. 2023. How the Birch effect differs in mechanisms and magnitudes due to soil texture. *Soil Biology and Biochemistry* 179 (2023), 108973.
- [89] Meera Stephen, Ali Nawaz, Sang Yeon Lee, Prashant Sonar, and Wei Lin Leong. 2023. Biodegradable materials for transient organic transistors. *Advanced Functional Materials* 33, 6 (2023), 2208521.
- [90] Emilius Sudirjo, Pim De Jager, Cees JN Buisman, and David PBTB Strik. 2019. Performance and long distance data acquisition via LoRa technology of a tubular plant microbial fuel cell located in a paddy field in West Kalimantan, Indonesia. *Sensors* 19, 21 (2019), 4647.
- [91] Natalia F Tapia, Claudia Rojas, Carlos A Bonilla, and Ignacio T Vargas. 2017. Evaluation of Sedum as driver for plant microbial fuel cells in a semi-arid green roof ecosystem. *Ecological Engineering* 108 (2017), 203–210.
- [92] Matteo Tucci, Carolina Cruz Viggì, Abraham Esteve Nunez, Andrea Schievano, Korneel Rabaey, and Federico Aulenta. 2021. Empowering electroactive microorganisms for soil remediation: Challenges in the bioelectrochemical removal of petroleum hydrocarbons. *Chemical Engineering Journal* 419 (2021), 130008.
- [93] Brendan L Turner, Jack Twiddy, Michael D Wilkins, Srivatsan Ramesh, Katie M Kilgour, Eleo Domingos, Olivia Nasrallah, Stefano Menegatti, and Michael A Daniele. 2023. Biodegradable elastomeric circuit boards from citric acid-based polyesters. *npj Flexible Electronics* 7, 1 (2023), 25.
- [94] María L Vera, Walter R Torres, Claudia I Galli, Alexandre Chagnes, and Victoria Flexer. 2023. Environmental impact of direct lithium extraction from brines. *Nature Reviews Earth & Environment* 4, 3 (2023), 149–165.
- [95] Jun Wang, Huan Deng, Shao-Song Wu, Yong-Cui Deng, Li Liu, Cheng Han, Yun-Bin Jiang, and Wen-Hui Zhong. 2019. Assessment of abundance and diversity of exoelectrogenic bacteria in soil under different land use types. *Catena* 172 (2019), 572–580.
- [96] Yuyang Wang, Ye Chen, Qing Wen, Hongtao Zheng, Haitao Xu, and Lijuan Qi. 2019. Electricity generation, energy storage, and microbial-community analysis in microbial fuel cells with multilayer capacitive anodes. *Energy* 189 (2019), 116342.
- [97] Samuel C.B. Wong, Sivert T. Sliper, William Wang, Alex S. Weddell, Stephanie Gauthier, and Geoff V. Merrett. 2020. Energy-Aware HW/SW Co-Modeling of Batteryless Wireless Sensor Nodes. In *Proceedings of the 8th International Workshop on Energy Harvesting and*

- Energy-Neutral Sensing Systems (ENSsys '20)*. Association for Computing Machinery, New York, NY, USA, 57–63. <https://doi.org/10.1145/3417308.3430272>
- [98] Jiawei Yang, Shaoan Cheng, Peng Li, Haobin Huang, and Kefa Cen. 2019. Sensitivity to oxygen in microbial electrochemical systems biofilms. *Iscience* 13 (2019), 163–172.
- [99] Zong-Chuang Yang, Yuan-Yuan Cheng, Feng Zhang, Bing-Bing Li, Yang Mu, Wen-Wei Li, and Han-Qing Yu. 2016. Rapid detection and enumeration of exoelectrogenic bacteria in lake sediments and a wastewater treatment plant using a coupled WO₃ nanoclusters and most probable number method. *Environmental Science & Technology Letters* 3, 4 (2016), 133–137.
- [100] Bao Yu, Liu Feng, Yali He, Lei Yang, and Yu Xun. 2021. Effects of anode materials on the performance and anode microbial community of soil microbial fuel cell. *Journal of Hazardous Materials* 401 (2021), 123394.
- [101] Daxing Zhang, Yubing Ge, and Weidong Wang. 2013. Study of a terrestrial microbial fuel cell and the effects of its power generation performance by environmental factors. In *Proceedings of the 2013 International Conference on Advanced Mechatronic Systems*. IEEE, 445–448.
- [102] Feiying Zhang and Hepeng Li. 2022. Effects of landscape restoration on migration of lead and cadmium at an abandoned mine site. *Frontiers in Environmental Science* 10 (2022), 1057961.
- [103] Fang Zhang, Jia Liu, Ivan Ivanov, Marta C Hatzell, Wulin Yang, Yongtae Ahn, and Bruce E Logan. 2014. Reference and counter electrode positions affect electrochemical characterization of bioanodes in different bioelectrochemical systems. *Biotechnology and bioengineering* 111, 10 (2014), 1931–1939.
- [104] Huajie Zou, Fuhai Cai, Jianghua Zhang, and Zhenyu Chu. 2022. Overview of environmental airflow energy harvesting technology based on piezoelectric effect. *Journal of Vibroengineering* 24, 1 (2022), 91–103.

A APPENDIX:

A.1 Soil Sample Report

The following soil sample testings were performed throughout the experiments described in Section 3.

Table 5. Soil classification results.

Analysis	Result	Unit	Method
Carbon, Total (C)	4.33	%	MSA Part 3 (1996) pp 963-977
Sand	53	%	Bouyoucos 1962
Silt	22	%	Bouyoucos 1962
Clay	25	%	Bouyoucos 1962
Soil Textural Classification	Sandy Clay Loam		USDA-NRCS

Table 6. Total organic carbon measurements from samples taken at each of the cells’ anode and the bulk soil after the v0 vs. v3 cell experiment featured in Figure 8. The anode soil samples were scraped directly from those respective carbon felt anodes while the bulk soil samples were collected at the specified locations.

Sample #	Description	Total Organic Carbon (%)
1	Cell 0 anode, v3	4.24
2	Cell 1 anode, v3	4.25
3	Cell 2 anode, v3	3.90
4	Cell 3 anode, v0	4.42
5	Cell 4 anode, v0	4.03
6	Cell 5 anode, v0	4.02
7	Bulk soil taken from between Cell 0 and Cell 3 at v0 anode depth	4.51
8	Bulk soil taken from between Cell 2 and Cell 5 at v3 anode depth	6.93

Table 7. Testing results from a soil sample collected at the end of the v2 experiments. The tests were performed by A&L Great Lakes Laboratories, and the same soil is used throughout the v1-v3 experiments described in Section 3.

Parameter	Value
Organic Matter (%)	5.9
Bray-1 Equiv. Phosphorus (ppm)	26
Potassium (ppm)	150
Magnesium (ppm)	560
Calcium (ppm)	2200
Sodium (ppm)	16
Soil pH	7.4
CEC (meq/100g)	16.1
Cation Saturation (% K)	2.4
Cation Saturation (% Mg)	28.9
Cation Saturation (% Ca)	68.2
Cation Saturation (% Na)	0.4
Soluble Salts 1:2 (mmho/cm)	0.2

A.2 SMFC Experimental Guide

A.2.1 Constructing SMFCs. This section details how one can build their own v3.1 soil microbial fuel cell (SMFC), which is more robust to low soil moisture levels compared to the MudWatts-like v0 design and will produce energy for longer, even during dry spells. Information regarding the function and conception of v3.1 and v0 cells can be found in Sections 3 and 5.2. We also go over how to construct the v0 cells so others can explore this popular design from literature. Both of these cells can be built from commercially available, off-the-shelf materials and 3D-printed parts with no advanced tools or processing.

Materials:

The bill of material is detailed in Table 8. Note that each v3.1 SMFC and v0 cell will require an approximately **25.4 x 12.7 cm** piece of PAN graphite felt for their two electrodes. Each v3.1 SMFC will also require a **10.7 x 12.5 cm** piece of 30% wetproofed carbon cloth.

Table 8. Bill of material for v3.1 and v0 SMFCs.

Item	Description	Quantity	URL
Carbon Cloth Wet Proofed (30% wetproof, 40 x 45 cm)	Gas diffusion membrane	1	Fuel Cell Store
J-B Weld 31310	Gasket/sealant for front panel	1	Amazon
All-Purpose RTV Silicone Sealant			
PAN Graphite Felt (6.3 mm thick, 40 cm x 40 cm)	Electrode material	1	Fuel Cell Store
TI5548	Connect electrode and load	1	Advent Research Materials
Titanium Insulated Wire			

Tools:

- 3D printer (standard FDMs that use PLA filaments such as Ultimaker 2+ or Prusa will work, and it should have a maximum print dimension greater than **15 x 15 x 18 cm** to accommodate the scaffold)
- Knife and ruler
- Pair of gloves (recommended for handling PAN graphite felt, which can irritate sensitive skin when dry)

Construction Procedure:*3D Printing:*

Access the Flange.stl, G_clip.stl, Scaffold_v3_1.stl, and Scaffold_v0.stl files from [GitHub](#). Load them into a slicing software to generate G-code files for 3D printing. You will need to print 1 flange, 1 scaffold, and 4 G-clips for each v3.1 SMFC, and 1 scaffold and 8 G-clips for each v0 SMFC. Refer to [Table 9](#) and [Table 10](#) for the printing specifications of these files.

Table 9. v3.1 cell 3D printing specifications.

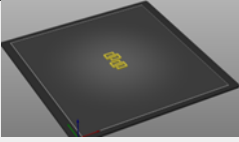
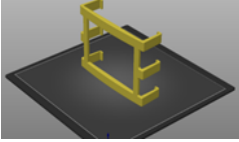
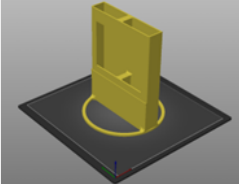
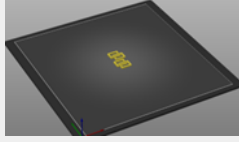
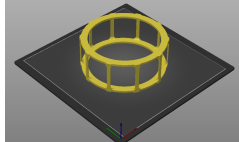
Item	# Parts	Orientation	Infill (%)	Fill Pattern	Nozzle Size (mm)	Support	Build Plate Adhesion
G_clip.stl	4		40	Triangle	<0.1	None	Skirt
Flange.stl	1		40	Triangle	<0.1	Everywhere	Skirt
Scaffold_v3_1.stl	1		40	Triangle	<0.1	Everywhere	Skirt

Table 10. v0 cell 3D printing specifications.

Item	# Parts	Orientation	Infill (%)	Fill Pattern	Nozzle Size (mm)	Support	Build Plate Adhesion
G_clip.stl	8		40	Triangle	<0.1	None	Skirt
Scaffold_v0.stl	1		40	Triangle	<0.1	None	Skirt

Cut Electrodes and Gas Exchange Membrane:

Follow the instructions below for v3.1 cell:

- (1) Put on some gloves prior to working with the PAN graphite felt to avoid skin irritation. Cut 1 piece of **12.7 cm** diameter disk from the PAN graphite felt stock using a knife. One can trace the outside of the ring on the scaffold to cut out a round disk that fits very closely. This is the anode.
- (2) Cut out a **10.7 x 12.5 cm** rectangle from the graphite felt stock using the knife and ruler. This is the cathode.
- (3) Cut a **10.7 x 12.5 cm** rectangle out of the 30% wetproofed carbon cloth. This should be the same size as the cathode cut in **Step 2**. This is the gas exchange membrane.

For v0 cell, simply follow **Step 1** twice to cut out the two identical felt disks required for the v0 electrodes.

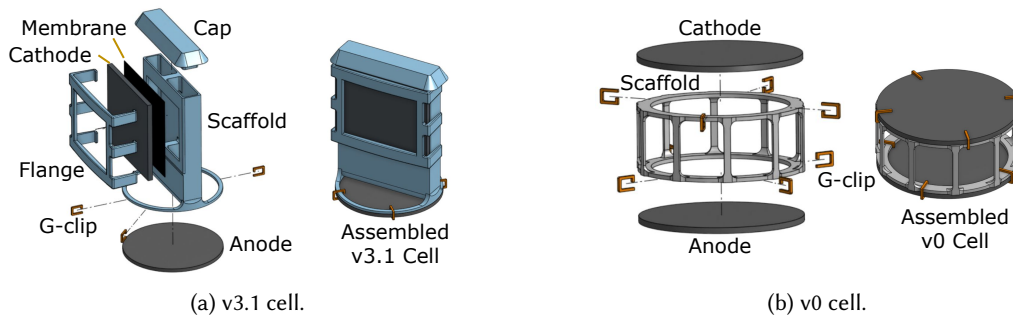
Assembly:

Fig. 26. Exploded and assembled view of two different SMFC designs with labeled components.

For v3.1 cell, follow the instructions below and pay close attention to the components in the cell (see [Figure 26a](#)):

- (1) Lay the scaffold down on a table so that the large window opening is facing up. Generously apply an even amount of silicone to the face of the scaffold, especially near the edge of the center window.
- (2) Place the gas exchange membrane over the window and push it down onto the scaffold. Make sure to line up the bottom of the membrane to the top of the protrusion below the scaffold window. Run a finger over the edges to smooth out the silicone.
- (3) Place the cathode graphite felt on top of the gas exchange membrane.
- (4) With both hands, pry the flange legs open just enough to fit them on the side of the scaffold. Line the bottom of the flange up to the bottom of the cathode so that they perfectly overlap, and push the flange into the scaffold until the 6 snap-fit legs lock behind the scaffold.
- (5) Wait 24 hours for the silicone to cure.
- (6) Put the cell into a container filled with water and rest a heavy object on top to prevent it from floating. Leave it in there for a couple of hours, and observe whether there is water in the air chamber. If there is water, remove the flange, cathode, and gas exchange membrane. Scrape off all silicone on the scaffold and repeat **Steps 1-5** with a new gas exchange membrane.
- (7) Now that the SMFC is confirmed to be watertight, put the anode under the ring, and secure it using at least four 3D printed G-clips (see [Figure 26a](#)).
- (8) Place the cap on the opening on top of the scaffold. This will ensure that rainfall and debris do not enter the air chamber.
- (9) Strip at least 5 cm of titanium wire and insert it well into the anode. Repeat this for the cathode. The ends of the wire will connect to the SMFC's load with the anode being ground and the cathode being power.

For the v0 cell, simply clip one of the graphite felt disks onto the scaffold with 4 clips exactly like in **Step 7** above (see [Figure 26b](#)). Insert the titanium wires into each electrode per **Step 9**. Leave the other electrode off the scaffold for now, since the inside of the cell needs to be filled with soil to form the electrolyte prior to installation.

A.2.2 Incubating SMFCs in Lab. This section details the procedure for incubating the v3.1 and v0 SMFCs so they may be experimented on in the lab or transplanted outside.

Supplies Needed:

To set up the incubation enclosure, one should have the following supplies:

- Large waterproof container capable of holding all of the desired sensors and cells while keeping sufficient distance between them. This is the incubation container, and it should support a minimum of 22 cm of soil depth for the v3.1 cell, and 10 cm for the v0 cell. It should also be strong enough to not bow or break under the weight of the wet soil and contain only inert materials to prevent altering soil chemistry.
- Wide and shallow containers for air-drying soil. Disposable aluminum pans for baking is an inexpensive option for this application. They should provide sufficient volume to hold all of the soil one wants to put in the large bin.
- Small shovel to mix soil.
- 10 mm sieve to homogenize and remove large particles from the soil. A larger/smaller sieve size may be used depending on the desired soil texture for the experiment.
- Mortar and pestle (or equivalent) to grind up large clumps of soil.
- Pair of garden gloves for protection from potential sharp objects in the soil.
- Ample soil to fill the large container even after grinding and sieving out large particles.
- Large plastic tarp capable of covering the top of the waterproof container to reduce the speed of evaporation. Note that it should not completely seal the container, as the cathodes require oxygen to function.
- Dionized/distilled water to hydrate the soil without introducing contaminants that can alter it.
- The user's choice of data logging equipment. Should be accurate to ± 1 mV for voltage measurements and ± 1 μ A for current measurements due to the SMFC's low output. This work used a 16-bit ADC (ADS1115) for voltage measurements on constant loads and leveraged Ohm's Law to calculate power, and the RocketLogger [85] for voltage and current measurements on loads with variable impedance (e.g., MARS). Additional monitoring sensors can be installed in the enclosure depending on the user's needs.

Soil Preparation:

- (1) Secure whatever soil one desires to incubate the SMFCs with and pick out any large debris.
- (2) Spread out the soil in the wide shallow containers and leave it to air dry in a ventilated area.
- (3) Once the soil is dried, grind it up into small particles using the mortar and pestle or whatever grinding equipment is available.
- (4) Sieve the soil to remove larger debris that can reduce the uniformity of the soil.
- (5) Once all the soil is processed and sieved, store it in a dry location until deployment.

Installing SMFCs (v3.1 with v0):

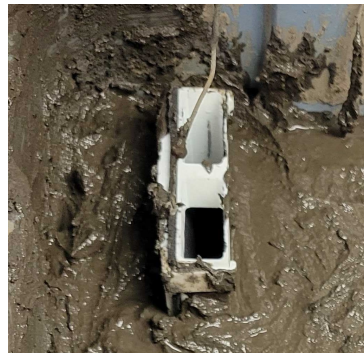
Below are the recommended steps to install the SMFCs in the waterproof container for incubation. These may be modified depending on the need of the experiment, and specific soil sensors (O_2 , soil moisture, temperature, etc.) can be installed at their desired locations as long as they do not interfere with the cells.

- (1) Saturate the newly sieved soil with dionized/distilled water. Mix very well until the soil becomes a slurry. Break up any clumps that formed while the soil was in storage. This will take a considerable amount of water, and it is extremely important to mix the soil very well at this step.
- (2) Fill the bottom of the large waterproof container with 5 cm of the wet soil slurry first.

- (3) Place the v3.1 SMFCs into the container with the anode side firmly pressed into the soil. Check that all v3.1 SMFCs are buried at the same depth. It may be helpful to use a level to check that one cell is not buried deeper than the other. The cells should also be spaced apart so they are not touching (see [Figure 27a](#)).
- (4) Fill up the enclosure with the soil slurry until the soil line is about 6 cm from the top of the v3.1 cells
- (5) Procedures for filling up the enclosure:
 - (a) **If also installing v0 SMFCs:** Place the half-assembled v0 SMFCs with only one graphite disk attached into the enclosure. Make sure the graphite disk is on the bottom of the cell and touches the soil (this disk is the anode). Check that their respective titanium wires and G-clips are firmly attached. Fill up the enclosure with more soil until the soil line reaches the top of the v0 scaffold, then clip the other graphite disk onto each scaffold with at least 4 G-clips per cell. The volume between the v0 anode and cathode should be completely packed with soil. Push down on the cathodes to ensure that there is no gap between the felt and the soil underneath, but make sure that all of the v0 cells are at the same depth. Add some more soil around the v0 cathodes so that the top of the cathodes is flush with the soil surface. Ensure that the soil line is at the top of the v3.1 scaffolds as well.
 - (b) **If installing v3.1 SMFCs alone:** Continue filling up the enclosure with soil until the soil line reaches the top of the scaffold so that the whole cathode is buried. [Figure 27b](#) is an example of v3.1 cells buried too shallow.
- (6) Connect the ends of the titanium wires to their respective loads, and add enough water to the enclosure so that the soil is saturated.
- (7) Cover the top of the enclosure with plastic tarp to reduce evaporation, then monitor the cells over the next 1-2 weeks for electrical activity. SMFCs incubated fastest in fully inundated conditions, so add more water throughout the incubation period if needed. See [Figure 27c](#) for the final setup.



(a) **Step 3** of the procedure from **Installing SMFCs**. The cells are spaced apart to ensure they are not touching, and there is about 5 cm of soil underneath the anodes.



(b) Example of an improperly installed v3.1 cell where the exposed side of the cathode is not completely buried. This will lower the effective cathode surface area for ion exchange, reducing the potential output of the SMFC.



(c) Cells 0-2 are the new v3.1 cells while cells 3-5 are the v0 control cells. The same configuration was used for the v2 and v3 cells in [Section 3](#).

Fig. 27. Experimental setup photos.